Palaeogeography, Palaeoclimatology, Palaeoecology 647 (2024) 112214

Contents lists available at ScienceDirect

Palaeogeography, Palaeoclimatology, Palaeoecology

journal homepage: www.elsevier.com/locate/palaeo

Plant cuticle as a possible palaeo-Hg proxy: Implications from Hg concentration data of extant *Ginkgo* L. and extinct ginkgoaleans

Li Zhang [a,b], Yongdong Wang [a,c,*], Micha Ruhl [b,**], Emma Blanka Kovács [b], Yuanyuan Xu [a,d], Yanbin Zhu [a,d], Ning Lu [e], Hongyu Chen [a,d]

[a] State Key Laboratory of Palaeobiology and Stratigraphy, Nanjing Institute of Geology and Palaeontology, Chinese Academy of Sciences (CAS), Nanjing 210008, China
[b] Department of Geology & Earth Surface Research Laboratory (ESRL), Trinity College Dublin, The University of Dublin, College Green, Dublin 2, Ireland
[c] Nanjing College, University of Chinese Academy of Sciences, Nanjing 210006, China
[d] University of Chinese Academy of Sciences, Beijing 10049, China
[e] College of Paleontology, Shenyang Normal University, Shenyang 110034, China

ARTICLE INFO

Editor: Prof. S Shen

Keywords:
Gaseous mercury concentration
Foliar/cuticular Hg concentration
Ginkgoaleans
Fossil cuticles
Early Jurassic
Karoo-Ferrar Large Igneous Province

ABSTRACT

Vegetative leaves have long been considered a significant receiver of gaseous Hg in the atmosphere, offering the potential to passively monitor palaeo-atmospheric Hg concentrations; however, few constraints on this exist. In this study, we conduct Hg measurements on three *Ginkgo* leaf collections: i) modern leaves from ten sampling sites across China, ii) modern leaves collected monthly across one growing season in Nanjing (China), iii) fossil ginkgoaleans leaves from the Middle Jurassic (China). The results from this study reveal that the foliar Hg concentrations (with an average concentration of 61 ng·g^{-1}, $N = 272$) were higher than those observed in *Ginkgo* leaf samples previously studied from Ireland and the USA. Additionally, the leaf age and atmospheric Hg concentrations represent two primary factors impacting foliar Hg contents in *Ginkgo*. Hg concentrations in fossil cuticular samples (with an average concentration of 585.5 ng·g^{-1}) were observed notably higher than those in modern *Ginkgo* leaves (avg. 61 ng·g^{-1}) and sediments from the same layers (avg. 113 ng·g^{-1}). Considering possible Hg migration during fossilization, we suggested that the elevated Hg concentrations in fossil cuticles were attributed to both the retention of Hg in leaves and the loss of leaf content during fossilization. Based on 23 fossil ginkgoalean samples from 6 beds of the Dameigou section (spanning from the Early to the Middle Jurassic), Qaidam Basin, China, we detected a Hg anomaly through Hg concentrations in fossil cuticles during the presumed palaeo-volcanic event (the Karoo-Ferrar Large Igneous Province (LIP)). This preliminary test supports the notion that variations in Hg concentrations in fossil cuticle may potentially reflect the gaseous Hg changes in the Jurassic palaeo-atmosphere, triggered by LIP volcanism at this time. This finding highlights the possibility of using fossil plant cuticle as a Hg proxy of palaeo-atmospheric Hg loading.

1. Introduction

Mercury (Hg) is a significant global contaminant that cycles between air, water, soil, and the biosphere and accumulates in the environment as a neurotoxic methylated compounds (MeHg) (Driscoll et al., 2013). MeHg can cause damage to the environment and human health (Hung et al., 2021; Laacouri et al., 2013). Human activities and natural processes release gaseous Hg into the environment, including Hg evasion from soil and water bodies, wildfires, volcanoes, and geothermal sources (Feng et al., 2022; Hung et al., 2021; Schroeder and Munthe, 1998). Anthropogenic activities produce approximately 2000 tons of global Hg emissions annually (Pacyna et al., 2006), significantly increasing the amount of Hg in the atmosphere since the onset of the Industrial Revolution (Feng et al., 2022; Travnikov, 2005).

Monitoring atmospheric mercury fractions enables understanding on the fate of mercury in the environment. Atmospheric mercury comprises gaseous elemental mercury (Hg^0, GEM, ng·m^{-3}) (> 90%), gaseous oxidized mercury (GOM, pg·m^{-3}), and particulate-bound mercury

* Corresponding author at: Y. Wang, State Key Laboratory of Palaeobiology and Stratigraphy, Nanjing Institute of Geology, Chinese Academy of Sciences (CAS), Nanjing 210008, China.
** Corresponding author at: M. Ruhl, Department of Geology, Trinity College Dublin, The University of Dublin, College Green, Dublin 2 D02PN40, Ireland.
E-mail addresses: ydwang@nigpas.ac.cn (Y. Wang), ruhlm@tcd.ie (M. Ruhl).

https://doi.org/10.1016/j.palaeo.2024.112214
Received 12 July 2023; Received in revised form 11 April 2024; Accepted 16 April 2024
Available online 21 April 2024

(PBM, pg·m^{-3}) (Gustin et al., 2015; Schroeder and Munthe, 1998). Hg^0 has a lifetime of 0.5–2 years, while GOM and PBM last only hours to weeks via wet and dry deposition (Ariya et al., 2015; Murphy et al., 2006). Atmospheric mercury measurements have been made at various locations worldwide (Sprovieri et al., 2017; Sprovieri et al., 2010), and the observational network of atmospheric Hg in China has been expanding since the 2000s (Feng et al., 2022; Fu et al., 2008; Fu et al., 2021; Liu et al., 2019; Zhang et al., 2021; Zhu et al., 2012).

Leaves are a well-known intermediate sink for atmospheric Hg, observed through field studies (Laacouri et al., 2013; Rea et al., 2002), chamber-growth studies (Assad et al., 2016; Ericksen et al., 2003; Tang et al., 2021), and forest ecosystems observations (Feng et al., 2022; Jun Zhou et al., 2021; Ning Zhou et al., 2021). More than 80% of the total Hg in aboveground biomass accumulates in leaves (Ericksen et al., 2003). Hg in leaves is however only in a limited capacity sourced through the root system, (Arnold et al., 2018; Ericksen et al., 2003; Fleck et al., 1999; Peckham et al., 2019; Rutter et al., 2011; Stamenkovic and Gustin, 2009), and almost all Hg in foliar tissue originates from the atmosphere (Lodenius et al., 2003; Manceau et al., 2018; Jun Zhou et al., 2021; Ning Zhou et al., 2021; Liu et al., 2022). The potential for monitoring atmospheric Hg concentrations using modern vegetation leaves as a passive receptor is gaining attention (Lodenius et al., 2003; Tang et al., 2021; Manceau et al., 2018; Zhou et al., 2017).

The strong correlation between foliar Hg in vegetation leaves and gaseous Hg concentrations in the atmosphere prompts essential questions: (i) whether Hg can be preserved within fossil leaf samples; and (ii) whether the Hg concentrations within fossil leaves can serve as a proxy for gaseous Hg in the palaeo-atmosphere. Prior to the Anthropocene era, natural mercury (Hg) emissions were primarily attributed to volcanic activity (Bergquist, 2017; Grasby et al., 2019; Kovács et al., 2024; Percival et al., 2015; Ruhl et al., 2022; Shen et al., 2020), aligning with climate disturbances that led to dramatic changes in flora, and various morphologies in leaves and pollen (Slater et al., 2019; Jun Zhou et al., 2021; Ning Zhou et al., 2021; Jin et al., 2022; Shen et al., 2022b; Vajda et al., 2023, 2024). Changes in palaeo-atmospheric gaseous Hg levels, during the palaeo-volcainc events, may be recorded by fossil plant leaves; however, no data constrains on this exist to date.

Ginkgoales have a long fossil record, originating in the Mesozoic, and only one species of *Ginkgo biloba* L. exists today (Wang et al., 2017; Zhou, 1997). The Ginkgoales' sensitivity to climate changes makes them ideally suited to track past changes in climate and the environment, because of which they are commonly used in palaeo-climate studies (McElwain, 1998; Barclay and Wing, 2016; Beerling et al., 1998; Wang et al., 2014; Zhang et al., 2019; Zhang et al., 2023).

For this study, we combine and compare the chemical analyses of Hg concentrations in both modern *Ginkgo* leaves and fossil Ginkgoales leaves. The modern leaves originate from ten sites in China, and associated data is compared to local gaseous atmospheric Hg levels as well as environmental (temperature, humidity) conditions, to explore possible factors influencing foliar Hg concentrations in *Ginkgo* leaves. Early to the Middle Jurassic fossil ginkgoalean leaves originate from the Dameigou section in the Qaidam Basin, China, and were analysed for their Hg content, to assess possible Hg-diagenesis during fossilization and to test the feasibility of using fossil leaf (cuticle) Hg concentrations as a proxy for palaeo-atmospheric Hg.

2. Materials and methods

2.1. Materials

2.1.1. Modern *Ginkgo biloba* leaves

Two sets of modern *Ginkgo biloba* leaves were sampled. The first set was collected geographically across China, including the northeast (Chifeng, Chaoyang, Shenyang), northwest (Jinchang, Lanzhou),

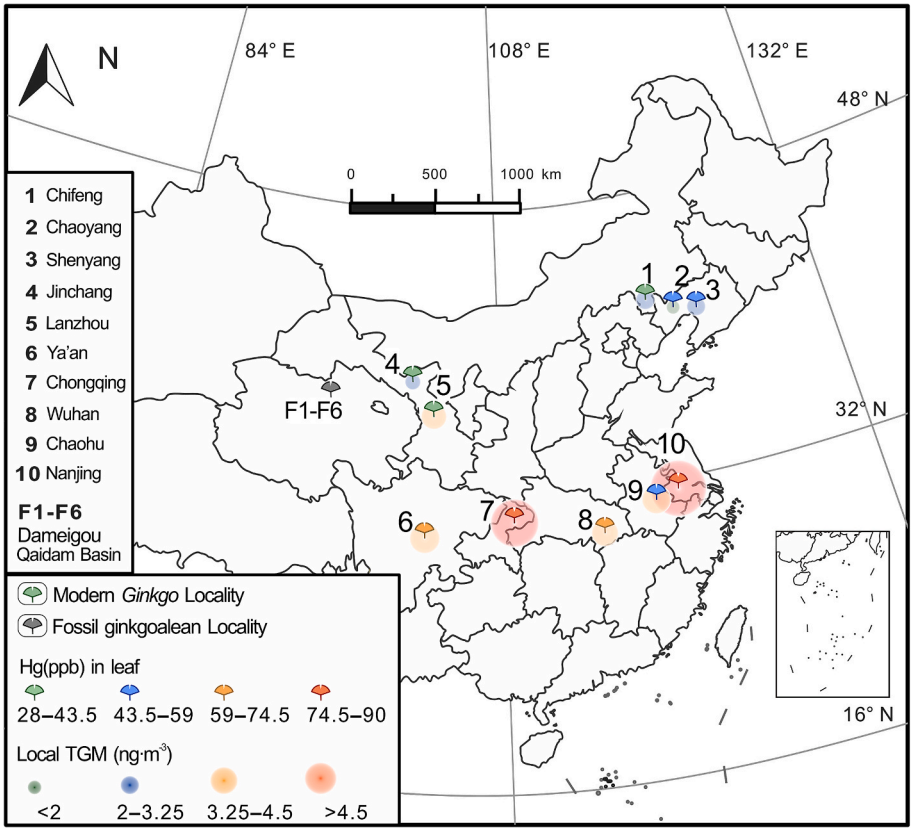

Fig. 1. Sampling sites of modern *Ginkgo biloba* L. and fossil ginkgoaleans. Mercury (Hg) concentrations in modern leaf samples and Local Total Gaseous Mercury (TGM) presented with different colours. Chinese basemap from the Standard Map Service, plan approval number: GS(2016)1595.

Table 1
Hg concentrations of *Ginkgo* leaf samples in China.

Samping sites	Hg % (ng·g^{-1})	Standard deviation	Sample amount	Environmental settings	Sampling Date
Set one - leaves collected spatially across China					
Nanjing(NJ)	91.38	11.3	16	Urban	19 Aug. 2020
Chongqing(CQ)	87.94	18.6	16	Field	27 Jul. 2020
Wuhan(WH)	73.27	13.7	16	Urban	13 Sept. 2020
Ya'an(YA)	72.70	5.5	16	Field	31 Oct. 2020
Chaohu(CH)	57.70	8.6	16	Urban	25 July. 2020
Shenyang(SY)	56.90	8.4	16	Urban	08 Sept. 2020
Chaoyang(CY)	55.00	9.8	16	Urban	20 Oct. 2020
Lanzhou(LZ)	31.18	6.8	16	Urban	25 July. 2020
Chifeng(CF)	30.24	4.3	16	Urban	26 July. 2020
Jinchang(JC)	28.31	6.7	16	Urban	15 Aug. 2020
Set two - leaves collected monthly in Nanjing (Jiangsu, China)					
Nanjing(NJ)	62.89	8.2	16	Urban	19 Jul. 2020
NJ	91.38	11.3	16	Urban	19 Aug. 2020
NJ	82.69	13.5	16	Urban	15 Sept. 2020
NJ	97.17	7.5	16	Urban	15 Oct. 2020
NJ	100.89	8.6	16	Urban	18 Nov. 2020
NJ	32.23	3.8	16	Urban	13 Apr. 2021
NJ	33.46	5.4	16	Urban	17 May. 2021
NJ	50.28	5.7	16	Urban	16 Jun. 2021

southwest (Ya'an, Chongqing), and southeast (Wuhan, Chaohu, Nanjing) (Fig. 1). Differing levels of industrial development in these cities have resulted in varying average gaseous atmospheric Hg concentrations (Feng et al., 2022; Fu et al., 2008; Fu et al., 2021; Liu et al., 2019) (Table S2). Sampled trees were distributed in urban and field settings (Table 1). The second set was collected monthly for one year (July–November 2020 and April–June 2021) from a *Ginkgo biloba* tree cultivated on the urban campus of the Nanjing Institute of Geology and Palaeontology, Chinese Academy of Sciences, China. All modern leaves were collected at a height of over two meters, and leaves were collected for each cardinal direction (North, East, South, West); also their position within the canopy (Sun, or Shade) was noted. In total, 136 foliar tissues were collected from 19 trees (Table S1).

Cuticle samples were extracted from modern *Ginkgo* leaves to investigate Hg concentration differences between bulk leaves and leaf-cuticle. Leaves with the highest (Nanjing, the November set), lowest (Jinchang), and middle (Chaohu) Hg concentrations (see Table 1) were selected for cuticle extractions.

2.1.2. Fossil ginkgoaleans

Twenty-three fossil ginkgoalean samples from six beds across three formations in the Dameigou section (Dameigou area, Qinghai, China) were collected for Hg analyses (Fig. 1). The sedimentary and geochemistry framework of the Dameigou section in the Qaidam Basin, China, have been described in previous studies, with the formations considered to span from the Early to the Middle Jurassic in age, constrained by palynological assemblages (Wang et al., 2005; Zhang et al., 1998) and carbon isotope chemostratigraphy (Lu et al., 2020; Zhou et al., 2022).

The ginkgoalean fossil cuticles analysed in this study include three common Mesozoic Ginkgoaceae foliage materials: *Ginkgoites*, *Sphenobaiera*, and *Baiera* (Table 2), with some of them sourced from previously reported samples (Li et al., 1988; Sze, 1959; Zhang, 2023; Zhang et al., 2023). In total, 23 ginkgoalean fossil leaf samples from six stratigraphically individual beds across three geological formations exposed within the Dameigou section (Qaidam Basin, China) were investigated in this study.

2.1.3. Biological materials archiving statement

Studied modern *Ginkgo* leaves were deposited at the State Key Laboratory of Palaeobiology and Stratigraphy, Nanjing, China and backed up at the Earth Surface Research Laboratory (ESRL), Trinity College Dublin, Ireland. Fossil ginkgoaleans studied here are deposited at the Palaeobotanical collection, Nanjing Institute of Geology and Palaeontology, Nanjing, China.

2.2. Methods

2.2.1. Cuticle extractions

Plant cuticle preparation for both modern and fossil samples studied was conducted at the Earth Surface Research Laboratory (ESRL), Trinity College Dublin, Ireland. For the modern *Ginkgo* leaf samples, they were treated with a solution of hydrogen peroxide (H_2O_2, 30%) + acetic acid (CH_3COOH, 95%) (1:1) in a 70 °C water bath for two to three hours until green samples became transparent. Following neutralization, the cuticle samples were dried using a vacuum pump.

Following traditional methods (Jones and Rowe, 1999), the fossil cuticle samples were treated with hydrochloric acid (HCl, 35%) and hydrofluoric acid (HF, 30%) to remove clay and siliceous rocks from the cuticles' surface, to ensure clean fossil cuticle sample material. To avoid any potential influence on the analysed Hg content, the fossil samples were not treated with nitric acid (HNO_3) throughout the preparation process. After neutralization, cuticle samples were transferred to filters, dried using a vacuum pump, and placed in clear test tubes.

2.2.2. Leaf Hg analysis

The study of total mercury concentrations in leaves was conducted at the Earth Surface Research Laboratory (ESRL), Trinity College Dublin, Ireland, with a LECO AMA-254 advanced mercury analyser, using the methodology described by Hall and Pelchat (1997) and Kovács et al. (2020). Because of the low weight of the samples (~ two to three miligrams on average), the analyses were run on 'blank-mode', resulting in absolute Hg quantity per sample. The relative concentration (ng·g^{-1}) was calculated offline. The ERM-CD281 (Rye Grass) reference material, with a certified value of 16.4 ng·g^{-1} (Centre et al., 2010), was repeatedly analysed to assess the precision of the Hg analyser. Duplicate Hg concentration analyses of a subset of the leaf samples were conducted (Table S1).

2.2.3. Elemental analyses of fossil samples

Elemental components of fossil cuticles were analysed using an energy-dispersive X-ray spectrometer (EDS). Total organic carbon contents (TOC) were measured with a Delta V isotope ratio mass spectrometer. These analyses were conducted at the State Key Laboratory of Palaeobiology and Stratigraphy, Nanjing Institute of Geology and Palaeontology, Chinese Academy of Sciences, in Nanjing, China.

Table 2
Hg concentrations, stomatal index, and assessed pCO_2 levels in fossil ginkgoaleans from the Dameigou section, Qaidam Basin, China.

Ser.	Stages	FM.	Fossil No.	Bed (Li et al., 1988)	Hg average (ppb ± SE.)	Stomatal Index (Zhang, 2023)	pCO_2 Variations Reconstructed by methods of i). SI-pCO_2 response curve (Barclay and Wing, 2016); ii). Carb. Std. (McElwain and Chaloner, 1996); iii). Mod. Std. (McElwain and Chaloner, 1996)*
Middle Jurassic	Bajocian-Aalenian	DMG.	F6	B-90	327.37 ± 57.2	5.35	790 – 1310
			F5	B-89	416.7 ± 70.4	4.22	950 – 1590
Lower Jurassic	Toarcian	YMG.	F4	B-58	701.7 ± 149.5	4.37	890 – 1490
			F3	B-56	619.9 ± 354.8	4.19	1010 – 1680
	Pliensb.	TSG.	F2	B-46	1215.6 ± 402.75	5.43	710 – 1190
			F1	B-38	670.63	5.13	750 – 1250

Abbreviations: pCO_2, CO_2 concentration; Ser., series; FM., formation; No., number; SE., standard errors; SI., Stomtal index; Carb. Std., carboniferous standard; Mod. Std., modern standard (Barclay and Wing, 2016; McElwain and Chaloner, 1996); DMG., the Dameigou formation; YMG., the Yinmagou formation; TSG., the Tianshuigou formation. *Systematics of fossil ginkgoaleans please refer to Zhang (2023). Given the scope of this study, more comprehensive fossil descriptions, stomtal parameters, and reconstructed paleo-CO_2 data will be released in a separate publication.

2.2.4. Atmospheric Hg data

The observational network of atmospheric Hg in China has been in development since the 2000s (Feng et al., 2022; Zhu et al., 2012). The latest datasets of local Total Gaseous Mercury (TGM) from sampling sites are available since the 2010s and were used to assess local atmospheric Hg levels; these were compared to modern leaf Hg concentrations analysed here (Table S2) (Feng et al., 2022; Fu et al., 2008; Fu et al., 2021; Liu et al., 2019; Zhu et al., 2012).

2.2.5. Statistical analysis

Least-square linear regression analysis was employed to constrain the possible relationships between *Ginkgo* foliar Hg concentrations and atmospheric Total Gaseous Mercury (TGM), Elevation (meters above sea level), Relative Humidity (mean value during the collecting month), Precipitation (accumulated precipitation in the collecting month), Temperature (mean value during the collecting month) (Table S2), as well as other relevant parameters. Polynomial regression analysis was utilized to model the relationship between Hg concentrations and leaf age. One-way analysis of variance (ANOVA) was applied to assess differences in Hg concentrations between leaves and cuticles, as well as between sun/shade leaves (Sokal and Rohlf, 1995).

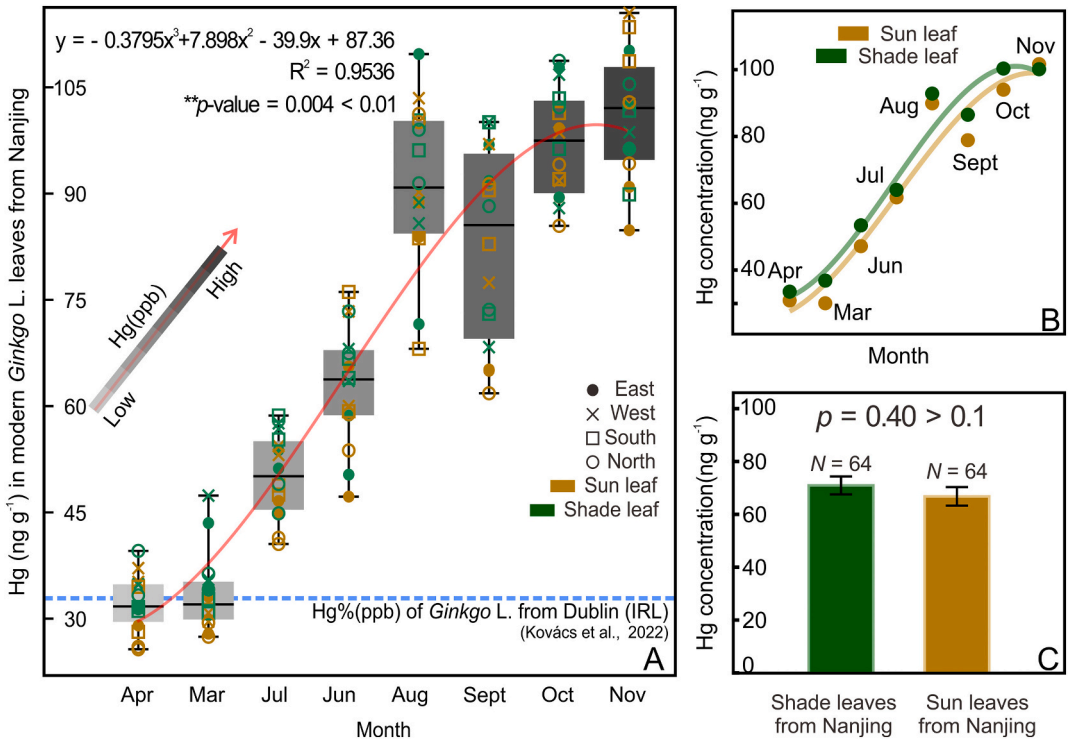

Fig. 2. Variations of *Ginkgo* foliar Hg concentrations across one growing season, based on a monthly-collected leaves from the same tree (Nanjing, China). (A) The boxplot shows foliar Hg concentrations gradually accumulated with leaf age, the blue dash line shows lower Hg concentrations in *Ginkgo* leaves from Dublin, Ireland, and the red line shows the polynomial correlation between foliar Hg concentrations and leaf age, $y_{(\text{Foliar Hg})} = -0.3795\ x^3_{\text{month}} + 7.898\ x^2_{\text{month}} - 39.9\ x_{\text{month}} + 87.36$, $R^2 = 0.95$, p-value = 0.004; (B) Significant polynomial correlations of foliar Hg concentrations against leaf age, established separately on data of Shade leaves (green) and Sun leaves (yellow), also showing slightly higher Hg concentrations in Shade leaves than those in Sun leaves; Statistics: $y_{(\text{shade-green})} = -0.428\ x^3_{\text{month}} + 8.85\ x^2_{\text{month}} - 45.7\ x_{\text{month}} + 100.7$, $R^2 = 0.96$, p-value = 0.0025; $y_{(\text{sun-yellow})} = -0.331\ x^3_{\text{month}} + 6.94\ x^2_{\text{month}} - 34\ x_{\text{month}} + 74$, $R^2 = 0.94$, p-value = 0.0065; (C) Variation of foliar Hg contents in *Ginkgo* between Shade leaves (green) and Sun leaves (yellow) in Nanjing, whereas the difference was not at stastistic level (p-value >0.1). (For interpretation of the references to colour in this figure legend, the reader is referred to the web version of this article.)

3. Results and discussion

3.1. Hg uptake by modern Ginkgo leaves

The main route of Hg exchange between plants and the atmosphere is via the uptake of Hg^0 by leaves (Jiskra et al., 2018; Lodenius et al., 2003). Studies conducted in growth chambers and in the field suggest that exposure to high vapour Hg concentrations leads to higher foliar Hg concentrations (Assad et al., 2016; Ericksen et al., 2003; Frescholtz et al., 2003; Lodenius et al., 2003; Manceau et al., 2018; Niu et al., 2011; Niu et al., 2013; Tang et al., 2021; Jun Zhou et al., 2020). Industrial activities have led to higher air Hg concentrations in sampling sites in China (ranging from 1.9 to 7.9 ng·m^{-3}), compared to on average lower background levels across the Northern Hemisphere (approximately 1.3–1.6 ng·m^{-3}) (Travnikov, 2005; Zhang et al., 2016). Under conditions of a high atmospheric Hg background, the uptake of Hg by vegetation is therefore expected to be higher, resulting in increased Hg concentrations within leaves (Zhou et al., 2018). Our *Ginkgo* dataset from China indeed displays higher foliar Hg concentrations (an average of 61 ng·g^{-1} for all samples, $N = 272$, see Table 1, S1) than other *Ginkgo* leaf samples collected from Trinity College Dublin, Ireland (roughly 20–30 ng·g^{-1}) (Kovács et al., 2022) (Fig. 2, A) and from the University of Minnesota, USA (19.1 ng·g^{-1}) (Laacouri et al., 2013).

Foliar uptake of Hg through stomata, has been proposed as the main process to enhance leaf Hg levels (Mosbæk et al., 1988). Stomatal conductance can be affected by a series of factors, including solar radiation intensity, ambient humidity and CO_2 conditions (Beerling et al., 1998; Herrick et al., 2004). This suggests that the position of leaves on a tree may have an impact on their foliar Hg concentrations. Therefore, it is essential to consider the different leaf positions within a tree when discussing the relationship between foliar Hg and atmospheric Hg to avoid potential discrepancies in understanding of the main controls on leaf Hg levels (Beerling et al., 1998; Herrick et al., 2004; Laacouri et al., 2013; Jun Zhou et al., 2021, Ning Zhou et al., 2021). Modern *Ginkgo biloba* leaves examined in this study were collected from multiple orientations, i.e. the North, East, South, and West cardinal directions, as well as both Sun and Shade positions within a tree. We utilized two sets of modern *Ginkgo* samples: (1) leaves collected monthly from Nanjing, China, and (2) leaves collected locally from ten different cities across China, reflecting regions with varying atmnospheric Hg levels. Based on these two sample sets, we explore the relationships of foliar Hg levels in *Ginkgo* leaves versus leaf age, atmospheric gaseous Hg (TGM), and other potential (environmental) forcing factors.

3.1.1. Leaf age and foliar Hg accumulation in Ginkgo across the growing season

Studies of different types of perennial angiosperms and gymnosperms provide evidence that plant leaves absorb and accumulate Hg^0 from the atmosphere (Ericksen et al., 2003; Laacouri et al., 2013; Lodenius et al., 2003; Jun Zhou et al., 2021; Ning Zhou et al., 2021). In our dataset, analysis of monthly collected *Ginkgo biloba* leaf samples from Nanjing (Table 1, S1), China, revealed an increasing trend in foliar Hg concentrations with leaf age over a growing season (Fig. 2, A–B). A close relationship between the foliar Hg concentrations and the leaf age was found by utilizing polynomial regression analysis ($y_{(\text{Foliar Hg})} = -0.3795 \cdot x^3_{\text{month}} + 7.898 \cdot x^2_{\text{month}} - 39.9 \cdot x_{\text{month}} + 87.36$, $R^2 = 0.95$, p-value = 0.004) (Fig. 2, A). These results indicate that *Ginkgo biloba* leaves consistently absorb and accumulate Hg during growth. Besides, the Hg uptake rates by leaves, represented by slopes of tangent lines along the curve, remain relatively stable during the growing to the mature stage (April–October) and decline only during the senescing stage (November) (Fig. 2, A–B).

3.1.2. Ginkgo foliar Hg concentrations under varying atmospheric backgrounds across China

The potential influence of spatial variations in airborne Hg levels on the foliar Hg contents in *Ginkgo biloba*, is here assessed through the analyses of modern leaf samples collected from ten localities across China, each marked with differing gaseous Hg concentrations (Fig. 1; Table 1, S1). Due to data availability and limitations, the total gaseous mercury (TGM) data were used to represent the approximate local atmospheric gaseous Hg levels (Table S2) (Fu et al., 2008; Fu et al., 2021; Liu et al., 2019). The results show significantly varying Hg concentrations among *Ginkgo biloba* leaves sampled from the different sites (Fig. 1; Fig. 3, A; Table 1). Specifically, we observe that foliar Hg concentrations in *Ginkgo biloba* leaves are higher in areas with high local atmospheric TGM levels: e.g. high Hg levels are observed in Nanjing (foliar Hg: 91.38 ng·g^{-1}; atmopsheric TGM: 7.90 ng·m^{-3}) and Chongqing (foliar Hg: 87.94 ng·g^{-1}; atmospheric TGM: 6.74 ng·m^{-3}), and low Hg levels are observed in Shenyang (foliar Hg: 56.90 ng·g^{-1}; atmospheric TGM: 2.63 ng·m^{-3}) and Chaoyang (foliar Hg: 55.0 ng·g^{-1}; atmospheric TGM: 1.93 ng·m^{-3}) (Fig. 3, A; Tables 1, S1).

In contrast to the variability of Hg in bulk leaves (from 20 to 110 ng·g^{-1}) (Table S1), the Hg contents in these cuticle samples are consistent, ranging from 20 to 25 ng·g^{-1} (Fig. 3, A; Table S1). This suggests that the acids (H_2O_2 + CH_3COOH) used in the cuticle extraction process may not completely remove all of the mesophyll tissue; this is supported by the fact that only 0.41 ng·g^{-1} of Hg was detected in modern *Ginkgo* cuticle samples (leaves were treated with dichloromethane, CH_2Cl_2) (Laacouri et al., 2013). However, the significant variance in Hg levels between bulk leaf and cuticle samples from modern *Ginkgo* leaves indicates that Hg is primarily distributed within mesophyll tissues rather than within the cuticles (Fig. 3, A; Table S1).

Due to the Hg accumulation with growth, leaf age can impact Hg concentrations in *Ginkgo* leaves (Fig. 2, A). The leaf samples were however collected locally in different months spanning from late July to late October, therefore observed foliar Hg concentrations should be corrected for the relative leaf age to make this comparison of data from different sites valuable. The leaf Hg correction assumes *Ginkgo* leaves to have absorbed Hg^0 at a consistent rate under individual atmospheric Hg levels, as well as at a higher rate in high-Hg^0 environments. We subsequently assessed and combined the presumed Hg uptake rate by *Ginkgo* ($Rate_{Hg\ uptake}$) and the leaf age bias (ΔT_{bias}, number of days), to assess the potential error in leaf Hg data ($Error_{Hg}$) due to collection at different months, between localities.

The empirical rate ($Rate_{Hg\ uptake}$) can be calculated by the monthly foliar Hg data (*Leaf Hg*) from the Nanjing sample and dataset spanning one entire growing season, using Eqs. (1)–(3) as follows:

$$Rate_{Hg\ uptake} = \frac{\Delta LeafHg}{\Delta T} \tag{1}$$

$$\Delta LeafHg = LeafHg_{Nov.} - LeafHg_{Jul.} \tag{2}$$

$$\Delta T = D_{Nov.} - D_{Jul.} \tag{3}$$

In Eqs. (2)–(3), the interval between mature–senescing stages of *Ginkgo* (Jul.–Nov.) were selected. Consequently, the difference of the foliar Hg concentrations during the period (Δ*Leaf Hg*) are 38 ng·g^{-1} (Eq. (2)) (Table 1), and the number of days (ΔT) of this period is 122 (Eq. (3)) (Table 1). With this, the presumed rate of Hg uptake by *Ginkgo* leaves during the mature–senescing stage was assessed to be 0.3115 ng·g^{-1}·d^{-1}, which was further used as the empirical rate of *Ginkgo* ($Rate_{Hg\ uptake}$) in the following calculations (Eqs. (4)–(6)).

$$LeafHg_{corrected} = Error_{Hg} + LeafHg_{observed} \tag{4}$$

$$Error_{Hg} = \Delta T_{bias} \times Rate_{Hg\ uptake} \times \frac{TGM_{local}}{TGM_{NJ}} \tag{5}$$

$$\Delta T_{bias} = D_{local} - D_{NJ} \tag{6}$$

The corrected foliar Hg concentrations ($Leaf\ Hg_{corrected}$) can be obtained by the sum of Hg errors ($Error_{Hg}$) and observed Hg data

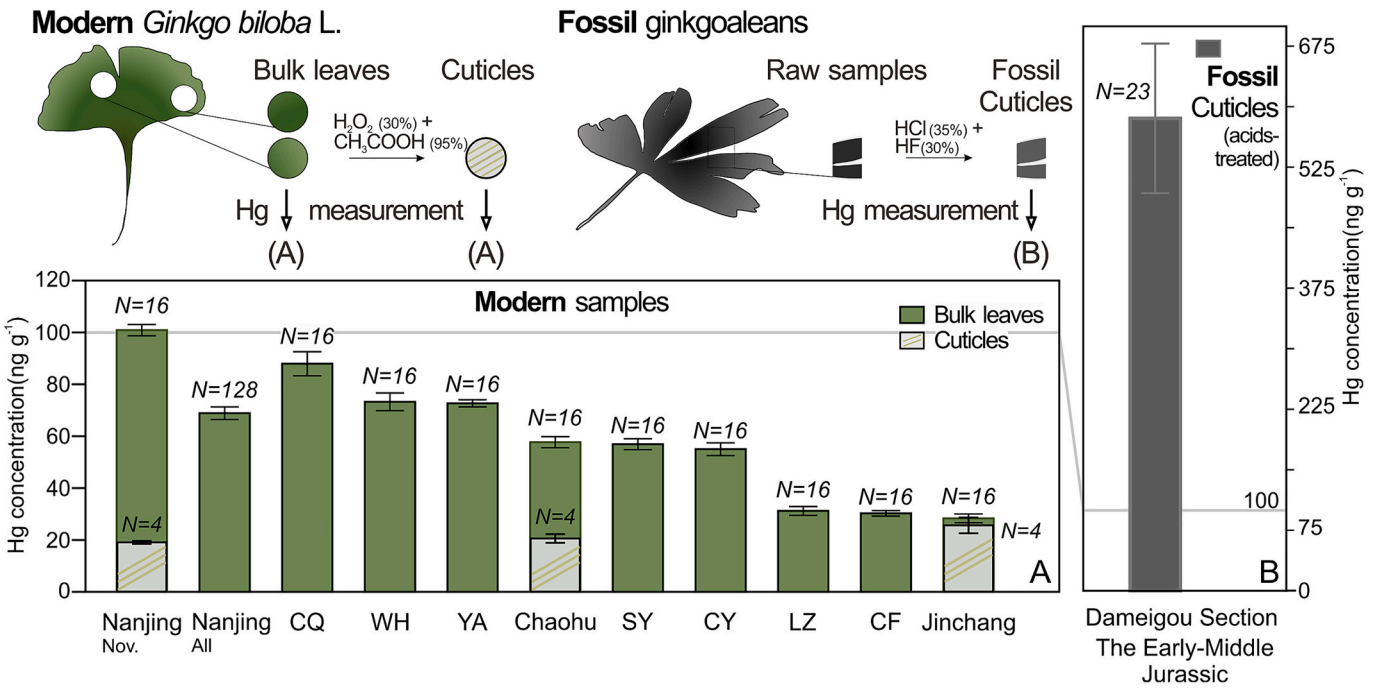

Fig. 3. Comparisons of Hg concentrations in modern and fossil samples. (A) Variations in Hg contents in leaf samples of *Ginkgo* from different sites in China, Hg concentrations in cuticle samples from three selected sites (shown in light gray boxes) show that Hg is mainly distributed within mesophyll tissues rather than cuticles; (B) Fossil cuticle samples contain higher Hg concentrations.

($LeafHg_{observed}$) (Eq. (4)) (Table 1, S2).

The Hg errors associated with leaf age ($Error_{Hg}$) can then be assessed using the leaf-age bias (ΔT_{bias}), and the $Rate_{Hg\ uptake}$ (Eq. (5)). Considering the probable variable $Rate_{Hg\ uptake}$ values of *Ginkgo* under spatially varying atmospheric Hg backgrounds states, the $Error_{Hg}$ was also weighted by the proportion of the local atmospheric TGM to the Nanjing atmospheric TGM $\left(\frac{TGM_{local}}{TGM_{NJ}}\right)$ (Eq. (5)). The leaf-age bias (ΔT_{bias}) is determined by the days' differences between the sampling dates of other regions (D_{local}) versus that of Nanjing (D_{NJ}) (Eq. (6)) (Table 1, S2). The date of 19th August (2020-08-19) was chosen as the D_{NJ}, because it is close to the average collection date of all samples (2020-08-27) (Table 1). For example, leaves sampled in Wuhan on the 13th of September (2020-09-13), have a 25-day (ΔT_{bias}) sample-delay compared to the leaves collected from Nanjing (2020-08-19); with this the $Error_{Hg}$ can be obtained as +7.43 ng·g^{-1} (Eqs. (5)–(6)), and the corrected Hg data can be calculated to be 76.8 ng·g^{-1} (Eq. (4)), with a five-percent positive offset in contrast to the original data (Table S2).

By utilizing the linear regression analyses, positive correlations were found between the Leaf Hg and the local atmospheric TGM ($y_{(LeafHg)} = 8.464 \cdot x_{TGM} + 23.9$, $R^2 = 0.64$, p-value <0.01) (Fig. 4, Fig. 5, A), and between the corrected Leaf Hg and the local atmospheric TGM ($y_{(Corrected\ LeafHg)} = 9.233 \cdot x_{TGM} + 22.7$, $R^2 = 0.58$, p-value <0.01) (Fig. 4, Fig. 5, A). These findings indicate that, besides the leaf age, the atmospheric Hg^0 content (here, interpreted to be represented by the atmospheric TGM) is another primary factor that affects the foliar Hg concentrations in *Ginkgo biloba*, similarly to other vascular plants (Assad et al., 2016; Ericksen et al., 2003; Frescholtz et al., 2003; Lodenius et al., 2003; Manceau et al., 2018; Niu et al., 2011; Niu et al., 2013; Tang et al., 2021; Jun Zhou et al., 2020, 2021; Ning Zhou et al., 2021).

3.1.3. Other factors affecting foliar Hg contents in Ginkgo

Recent studies have demonstrated that >89% of Hg uptake in plants occurs through gas exchange between leaves and the atmosphere (Ericksen et al., 2003; Lodenius et al., 2003; Manceau et al., 2018; Jun Zhou et al., 2021; Ning Zhou et al., 2021; Liu et al., 2022). The root uptake of Hg into plant tissue is minimal, and is indeed suggested to account for <10% (Arnold et al., 2018; Ericksen et al., 2003; Fleck et al., 1999; Peckham et al., 2019; Rutter et al., 2011; Stamenkovic and Gustin, 2009). Minimal root uptake was demonstrated by negligible uptake and translocation of Hg into tree tissue, from $HgBr_2$-spiked soils (mercury(II) bromide) (Arnold et al., 2018; Peckham et al., 2019), $HgCl_2$-spiked soils (mercury(II) chloride) (Stamenkovic and Gustin, 2009), or soils spiked by stable Hg isotopes (Graydon et al., 2009), as well as by the lack of an observable positive correlation between leaf Hg and soil Hg levels (Assad et al., 2016; Fleck et al., 1999; Gačnik and Gustin, 2023; Tang et al., 2021).

The dominant pathway for atmospheric Hg uptake by plant leaves is via stomata (Laacouri et al., 2013; Manceau et al., 2018; Wohlgemuth et al., 2020; Jun Zhou et al., 2021; Ning Zhou et al., 2021). Stomatal uptake refers to the process of physical diffusion and biochemical fixation of Hg^0 from the atmosphere into leaf interior tissues (Gačnik and Gustin, 2023; Laacouri et al., 2013; Liu et al., 2022; Naharro et al., 2020; Stamenkovic and Gustin, 2009). There is strong evidence, including from our modern *Ginkgo* dataset, that Hg stored in foliage is significantly and positively influenced by leaf age (Fig. 2) (Assad et al., 2016; Ericksen et al., 2003; Laacouri et al., 2013) and atmospheric Hg concentration levels (Fig. 4; Fig. 5, A) (Naharro et al., 2020; Stamenkovic and Gustin, 2009).

Other environmental factors have also been suggested to potentially affect the Hg accumulation in foliage, such as local humidity, precipitation, temperature (Haworth et al., 2018; Wohlgemuth et al., 2022; Zhang et al., 2023; Jun Zhou et al., 2021; Ning Zhou et al., 2021), sunlight intensity (Liu et al., 2022; McAusland et al., 2016; Naharro et al., 2020) and elevation (McElwain, 2004; Xu et al., 2020). These abiotic parameters may cause variations in foliar Hg uptake and concentration by affecting the leaf physiological characteristics such as stomatal number (Haworth et al., 2018; Laacouri et al., 2013), stomatal conductance (El-Sharkawy et al., 1985; Mosbæk et al., 1988; Naharro et al., 2020; Sun et al., 2003) and the rate of net photosynthesis (Teixeira et al., 2018; Jun Zhou et al., 2021; Ning Zhou et al., 2021; Liu et al., 2022; Gačnik and Gustin, 2023). The net photosynthesis rate may

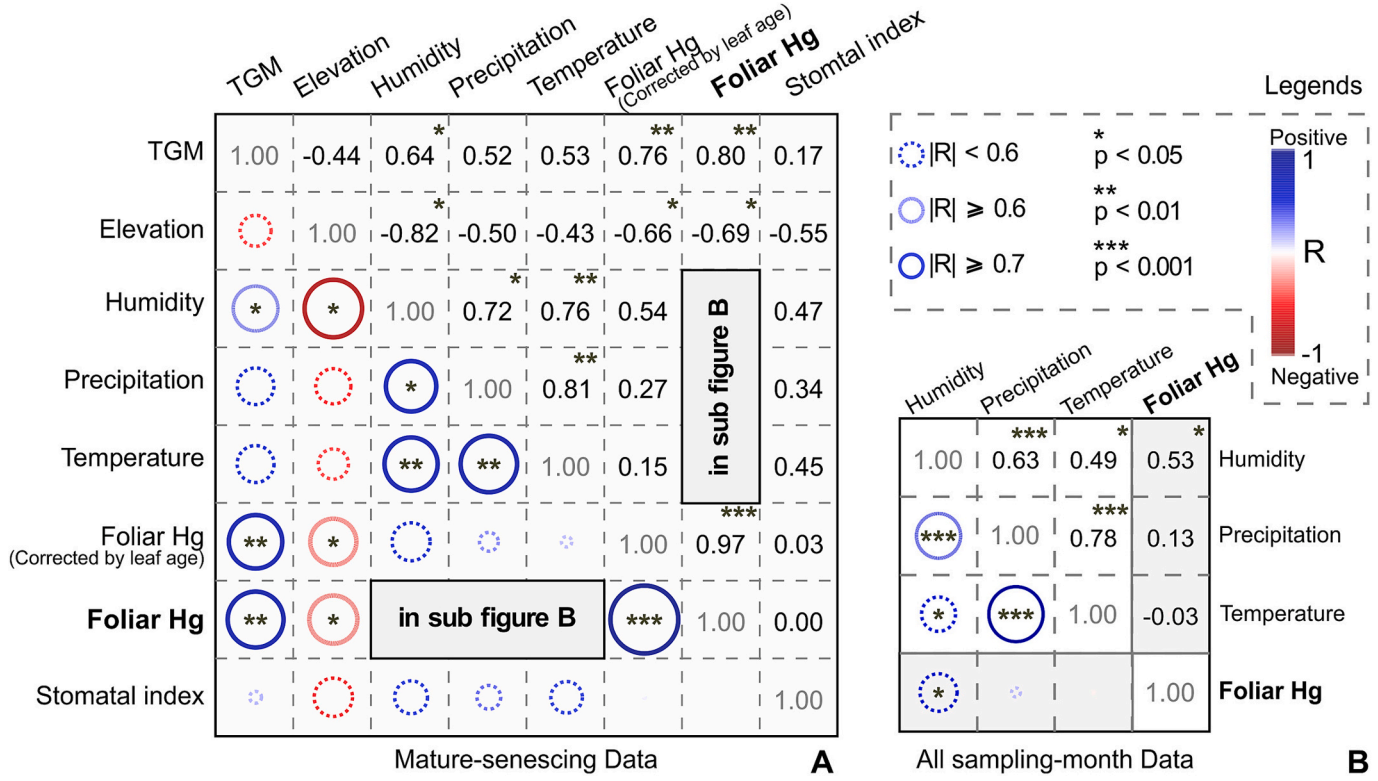

Fig. 4. Correlation plots illustrating potential relationships between biotic variables of *Ginkgo* and abiotic parameters (A). The relationships between foliar Hg contents in *Ginkgo* and monthly climate parameters are presented in (B). In correlation plots, the upper half of the figures give correlation coefficients (R-values) for each pair of variables, and were illustrated by blue (positively-correlated) and red (negatively-correlated) circles in the lower half. Significant correlaions were marked by *($p < 0.05$), **($p < 0.01$), and ***($p < 0.001$). *Parameters*: TGM, Total Gaseous Mercury ($ng{\cdot}m^{-3}$); Elevation, meters above sea level (m); Humidity, average relative humidity in collecting months (%); Precipitation, accumulated precipitation in collecting month (mm); Temperature, average values in collecting months (°C); Foliar $Hg_{(corrected\ by\ leaf\ age)}$, presumed foliar Hg data by leaf age correction ($ng{\cdot}g^{-1}$); Foliar Hg, observed foliar Hg data ($ng{\cdot}g^{-1}$); Stomtal index (%) from Zhang et al. (2023). All climatic parameters are available at the China Meteorological Data Service Centre/National Meteorological Information Centre (http://data.cma.cn). All data used can be found in Tables 1 and S1–S2. (For interpretation of the references to colour in this figure legend, the reader is referred to the web version of this article.)

however vary between species (Pandey et al., 2003; Teixeira et al., 2018); as this study exclusively focuses on *Ginkgo biloba*, this parameter is excluded from further consideration here. For the remaining abiotic environmental parameters listed above, we employed correlation plots and linear regression analyses to assess their potential relationship to the foliar Hg concentrations of the here studies on modern *Ginkgo biloba* leaf sample set (Figs. 4, 5).

Two of the main climatic parameters, *precipitation* (accumulated precipitation in the collecting month) (Fig. 4, B, Fig. 5, D) and *temperature* (average value during the collecting month) (Fig. 4, B, Fig. 5, E), show limited to no significant correlations with foliar Hg concentrations in *Ginkgo biloba*, whereas a positive correlation between *local relative humidity* and the foliar Hg concentrations was observed (correlation coefficient, $R = 0.53$, p-value <0.05) (Fig. 4, B, Fig. 5, B). This is in agreement with a previous study that was conducted on *Epipremnum aureum* (golden pothos) in a controlled laboratory setting (Naharro et al., 2020), also demonstrating an effect of relative humidity on foliar Hg assimilation.

Elevated altitudes also have the potential to affect Hg uptake by plants because a lower CO_2 partial pressure leads to a higher stomatal frequency in plant leaves, as demonstrated by observations in black oak (*Quercus kelloggii*) (McElwain, 2004). However, in our modern *G. biloba* dataset, we observe a negative correlation between foliar Hg concentrations and local altidtude (with $R = -0.66$, p-value <0.05) (Fig. 4, Fig. 5, C). In this case, we do not observe the stomatal index to match local elevation (p-value >0.05) (Fig. 4), suggesting a limited influence of elevation on stomatal characteristics in *Ginkgo* leaves (Xie et al., 2009; Steinthorsdottir et al., 2022; Zhang et al., 2023). Further studies may however be needed to explore the influence of elevation on foliar Hg levels.

Sunlight intensity is known to impact the stomatal development of plant leaves, as sun leaves developing in full sunlight around the outer edges of the crown tend to possess higher stomatal densities than shade leaves, which develop within the canopy (Boardman, 1977; Lange et al., 1981; Sun et al., 2003). The here studied sun leaves indeed exhibit slightly lower foliar Hg concentrations than shade leaves from the same trees (Fig. 2, B–C, Fig. 5, F). However, the observed difference in foliar Hg concentrations is not statistically significant (p-value >0.1), and within analytical uncertainty, suggesting that solar radiation intensity (interpreted from the analyses of sun/shade leaves here) has only limited to no effect on foliar Hg concentrations.

Combined, our data indicate that leaf age as well as atmospheric Hg concentrations are by far the strongest influence on *Ginkgo biloba* foliar Hg levels (Fig. 2) (Assad et al., 2016; Ericksen et al., 2003; Laacouri et al., 2013), both with values of $p < 0.01$ (Fig. 4, A, Fig. 5, A) (Naharro et al., 2020; Stamenkovic and Gustin, 2009). Additionally, relative humidity and elevation emerge as potential abiotic factors impacting on Hg levels in *Ginkgo biloba* leaves, but constraints on the exact relationship require further investigation ($p < 0.05$ for both) (Fig. 4, Fig. 5, B, C).

3.2. Hg in fossil cuticles of ginkgoaleans

Both field and chamber studies have consistently demonstrated a positive correlation between foliar Hg and atmospheric Hg (Fig. 4, A,

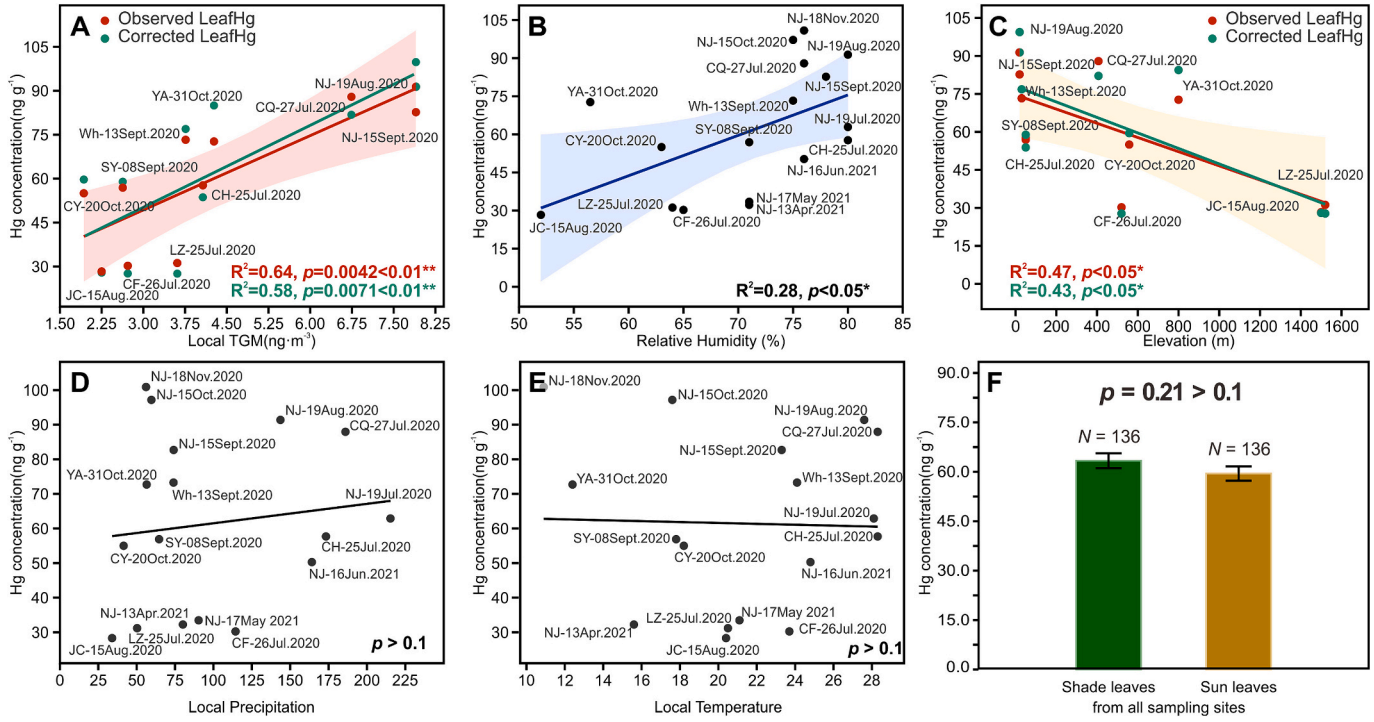

Fig. 5. Linear regressions of foliar Hg concentrations in *Ginkgo* versus (A) Total gaseous mercury (TGM), (B) Relative humidity (average values in collecting months), (C) Elevation (meters above sea level), (D) Precipitation (accumulated precipitation in collecting month), and (E) Temperature (average values in collecting months) (Table S2). Sub-fig. (F) shows the difference in Hg contents between Shade/Sun leaf samples from all Hg data (Table S1). The sampling dates of leaves were annotated. The coefficient of determination R^2 and *p*-value were listed respectively, and slope and 95% (2 s) biconcave confidence belts were given for those significant correlations ($p < 0.05$). The calibrations and parameters used for linear regression analyses in A–E are the same as in Fig. 4. *Location Abbreviations*: CH, Chaohu; CF, Chifeng; CQ, Chongqing; JC, Jinchang; LZ, Lanzhou; NJ, Nanjing; SY, Shenyang; WH, Wuhan; CY, Chaoyang; YA, Ya'an.

Fig. 5, A) (Gačnik and Gustin, 2023; Laacouri et al., 2013; Liu et al., 2022; Naharro et al., 2020; Stamenkovic and Gustin, 2009). Therefore, the feasibility of utilizing fossil foliar Hg as a potential proxy to reflect past atmospheric Hg levels is here evaluated. However, the preservation of Hg in fossil cuticle should be assessed before its use as indicator of past atmospheric Hg levels or fluxes. We therefore assessed the possible Hg sources in fossil cuticles from a taphonomic perspective.

3.2.1. *Possible sources of Hg in fossil cuticle (compressions)*

A plant cuticle is a non-cellular amorphous layer that is deposited on the outside and into the walls of the epidermal cells (Javelle et al., 2011; Riederer and Schreiber, 2001). Because the cuticle is inert and resistant to decay, it can be preserved in the sediment, and it represents a valuable source of palaeobotanical, biochemical and palaeoenvironmental information (Jardine et al., 2019; Lomax et al., 2019; McElwain and Chaloner, 1995, 1996; Steinthorsdottir et al., 2018; Vajda et al., 2017; Zhang et al., 2023).

In modern leaves, the majority of Hg is stored within mesophyll tissues rather than in the cuticles (Fig. 3, A), both in *Ginkgo biloba* (this study) and in other deciduous species (Laacouri et al., 2013). In contrast, fossil cuticular samples revealed high Hg concentrations (average 585.5 $ng{\cdot}g^{-1}$) (Fig. 3, B), which were nearly ten times higher than those in modern leaves (avg. 61 $ng{\cdot}g^{-1}$) (Fig. 3, B, Table 1–2) and five times higher than those in sediments from the same layers (avg. 113 $ng{\cdot}g^{-1}$) (Fig. 6, D) (Zhou et al., 2022).

To better understand the high Hg concentrations in fossil plant cuticular samples, we assess the formation process of compression-type fossils. Living plant foliage takes up Hg^0 from the atmosphere (Ericksen et al., 2003; Fleck et al., 1999). Following absorption, Hg will be fixed and held within the leaf tissue as forms of mercury sulfide nanoparticles (HgS_{NP}) and mercury-thiolate complexes (Hg-SR). (Manceau et al., 2018) (Fig. 6, A). We hypothesised that Mesozoic ginkgoaleans had a similar leaf Hg-uptake mechanism as their living relatives, i.e., Hg^0 in the palaeo-atmosphere would be absorbed and stored by the ginkgoaleans' leaves (Fig. 6, A). Typically, leaves decompose, and Hg in foliage will be released back into the environment (air, soil, and/or sediments) (Laacouri et al., 2013; Lu et al., 2021; Obrist et al., 2018; Zhou et al., 2018). However, a small fraction of fresh leaves may be preserved and become fossils at any given time.

As the result of mechanical removal or natural senescence, leaves fall and undergo transportation before burial (Arnold, 1947; Harris, 1976; Taylor et al., 2009; Zhang et al., 2022). The decay of the mesophyll tissue begins once the leaf falls and continues during transportation to low-energy aqueous depositinal environments (Rex and Chaloner, 1983; Rex, 1986). Mercury stored in a leaf may then be released into the environment in the form of oxidized mercury (Hg(II)) and MeHg during leaf decay by microbes (Laacouri et al., 2013; Lu et al., 2021; Obrist et al., 2018) (Fig. 5, B).

Simultaneously, upon the leaf entering the aqueous environment, the process of biofilm-clay formation on the leaf begins. This process protects the leaf from decay, enhancing leaf preservation and fossilization (Iniesto et al., 2018; Locatelli et al., 2017) (Fig. 6, C). The biofilm, or the biofilm-mediated clay accumulation during the process, absorbs Hg(II) and MeHg from the ambient environment (de Araújo et al., 2019; Gworek et al., 2020; Hintelmann et al., 1993; Zhu et al., 2015) (Fig. 6, C).

After compaction, and without exposure to elevated temperatures (< 25 °C), pressures (< 25 bar), or hydrothermal fluids, the leaf is preserved in the rock matrix as an organic-rich compression (Locatelli et al., 2017; Meyer, 2003; Retallack and Dilcher, 2012; Samuels et al., 2008). On the surface of the raw fossil cuticles, both organic elements (C, O) and clay mineral elemental components (e.g., Si, Al) can be detected by utilizing an energy-dispersive X-ray spectrometer (EDS) (Fig. 6, D). This suggests that the biofilm-mediated clay, a potential carrier of Hg, may be

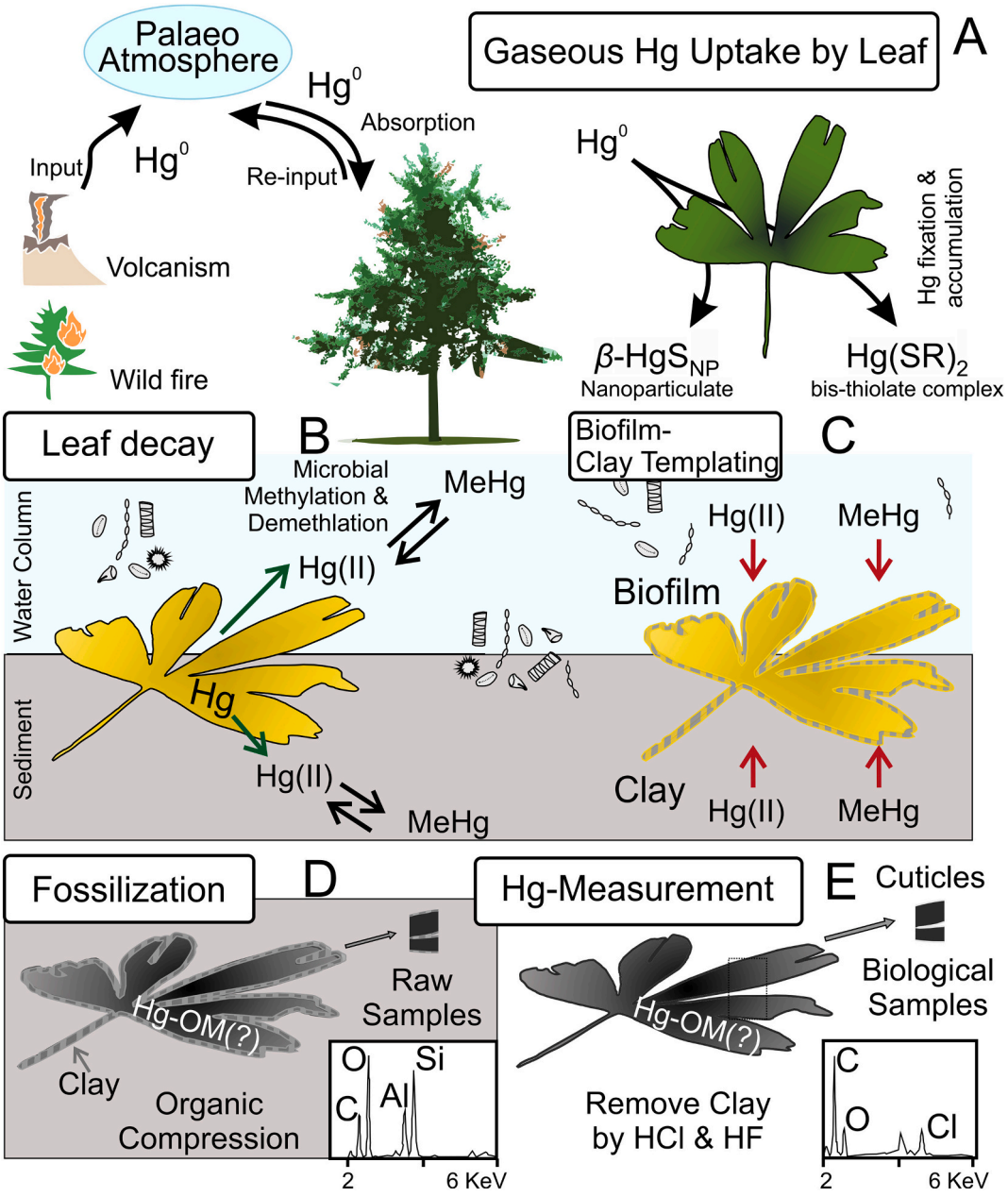

Fig. 6. Possible pathways of Hg migration in leaves during fossilization. (A) the uptake and fixation of Hg^0 by leaf, the Hg was stored in leaf as forms of mercury−sulfur nanoparticles (HgS_{NP}) and Hg(II)-thiolate complexes (Hg-SR) (Manceau et al., 2018); the natural sources of Hg^0 was suggested the palaeo-volcanism and palaeo-wild fires (Schroeder and Munthe, 1998; Bergquist, 2017; Kovács et al., 2020; Ruhl et al., 2022; Percival et al., 2015); (B) The leaf decay, during which a small fraction of the stored Hg in the leaf would be released into environment (Laacouri et al., 2013; Obrist et al., 2018; Locatelli et al., 2017; Lu et al., 2021; Zhou et al., 2018); (C) The formation of the biofilm-clay, during which both the biofilm and the biofilm-mediated clay absorb Hg from the environment (Zhu et al., 2015; Hintelmann et al., 1993; de Araújo et al., 2019; Gworek et al., 2020); (D) Compaction and diagenesis during fossilization; the clay around the fossil cuticle was detected by EDS (see Section 2.2.2); (E) Hg measurement of fossil cuticles, the clay was removed by the acid treatments of HCl and HF; and high concentrations of Hg within fossil cuticles was detected.

preserved on the fossil cuticle.

The hypothesised formation of compression-type leaf fossils, or fossil cuticle suggests that the main factors influencing Hg concentrations in fossil cuticular samples include: (1) Hg uptake by leaves from the palaeo-atmosphere when the plants were alive (Fig. 2; Fig. 5, A; Fig. 6, A); (2) the relative age of the leaf when it detached from the parent tree (Fig. 2; Fig. 5, A); (3) Hg loss during leaf decay (Fig. 6, B); (4) environmental Hg absorbed by the biofilm and clay (Fig. 6, C); and (5) leaf mass loss during fossilization (Fig. 6, D).

Mercury loss during leaf decay may be limited (Pokharel and Obrist, 2011; Zhou et al., 2018). Both in coniferous and broad-leaved forests over 90% of the litterfall Hg was in an inert fraction after a 1-year decomposition, therefore Hg concentrations in litterfall may be considered stable on shorter (1–2 year) timescales (Pokharel and Obrist, 2011; Zhou et al., 2018).

The influence of environmental Hg absorption by clay can also be constrained, as the acid treatment (HCl and HF) employed in our study removes the clay around fossil cuticle samples (Fig. 6, E). This conventional chemical treatment is necessary for total cuticle extraction, to preserve the biotic signals of fossil cuticles by removing inorganics (carbonates and silicates). While initially believed to minimally impact the physical structures and chemical components of fossil cuticles (Jones

and Rowe, 1999), recent findings suggest that HCl treatment may however result in a loss of a small fraction of the leaf organic matter (Cavalcante et al., 2023), which may lead to Hg loss in (fossil) leaf/cuticle when prepared for further analyses using such methodology. Although the Hg concentrations in acid-treated cuticle (thus, the biotic substrate) tends to be higher than those in raw (non-treated) cuticle substrates, we here use acid-treated cuticle materials for the analyses of original leaf Hg levels, because this methodology is the only way to ensure the full removal of (possibly Hg carrying) clay mineral coatings, with this likely providing a more accurate assessment of the Hg levels in the analysed fossil cuticle material. Currently, the speciation of Hg in fossil cuticle remains unknown; we here hypothesise that Hg in fossil cuticle is hosted by organic matter (OM), because of the biological and sedimentary nature of compression-type fossils. The here observed high Hg levels in fossil sample substrates (Table 2), indeed suggests that the likely OM-bound Hg in cuticle experiences only a limited to no impact from the utilized acid treatment. Hence, the elevated Hg concentrations observed here in fossil cuticles are likely predominantly attributable to the original leaf sequestration of Hg, combined with the relative leaf age (collectively summarized as Hg retention in leaves), and the mass loss of bulk leaves during fossilization. As similar conditions of fossil preservation may result in comparable losses of leaf mass in compression fossils, stratigraphic variations in Hg concentrations of fossil cuticle may still signify changes in Hg loading of the palaeo-atmosphere, despite fossil cuticle Hg contents possibly being offset from the original leaf Hg levels.

3.2.2. *Hg contents in fossil ginkgoaleans during palaeo-volcanism: a preliminary test*

Volcanism forms the largest natural source of gaseous Hg in the present-day atmosphere. The potential use of fossil cuticles to assess environmental/atmospheric Hg loading from past major volcanic events is here tested by the study of a major Jurassic global change event, the Toarcian Oceanic Anoxic Event (T-OAE), which coincided with Karoo-Ferrar large igneous province (LIP) volcanism. Here, we collected 23 ginkgoalean fossil leaf samples from six stratigraphically individual beds across three geological formations exposed within the Dameigou section (Qaidam Basin, China) (Fig. 7). The expanded and continuous sedimentary succession here, is bio- and chemostratigraphically well constrained and spans the Lower and Middle Jurassic, including the T-OAE (Li et al., 2014; Lu et al., 2020; Wang et al., 2005; Zhang et al., 1998; Zhou et al., 2022). Based on similar variations of carbon isotope excursions and Hg and Hg/TOC anomalies in sediment records in Dameigou (China) as those in Mochars (United Kingdom) (Ruhl et al., 2022) (Fig. 7, D), Zhou et al. (2022) suggested the paleoclimatic conditions during the Early Jurassic in the Dameigou area to have been affected by global environmental change instigated by emplacement of the Karoo-Ferrar LIP.

Mercury measurements on the fossil ginkgoalean samples (cuticles) collected from the Dameigou section as well as stomatal data obtained from the same set of ginkgoalean samples (Zhang, 2023) provide insight into Jurassic palaeoclimate variations, and it tests its possible link to environmental Hg loading and LIP volcanism at this time. Due to the fossil compressions/cuticles consisting purely of organic matter (Locatelli et al., 2017; Meyer, 2003; Retallack and Dilcher, 2012), the commonly applied Hg/TOC correction for bulk sediment samples (Percival et al., 2015; Shen et al., 2022a; Shen et al., 2022b) was not employed here. The analysed (acid-treated) fossil cuticle samples exhibit stable total organic carbon (TOC) values of 25–37% (Table S3).

The analysed fossil cuticles exhibit relatively high Hg concentrations, with an average of 585.5 ± 92.7 ng·g^{-1} (ppb ± SE). Across stratigraphy, the cuticle Hg concentrations range from 327 ng·g^{-1} at stratigraphic bed F6 (at the top of the Dameigou Formation, Fig. 7), to 1215 ng·g^{-1} at stratigraphic bed F2 (at the top of the Tianshuigou Formation) (Table 2; Fig. 7). The upper Pliensbachian beds F1 and F2 show higher and peak cuticle-Hg content (Table 2, Fig. 7, C), consistent with the results from

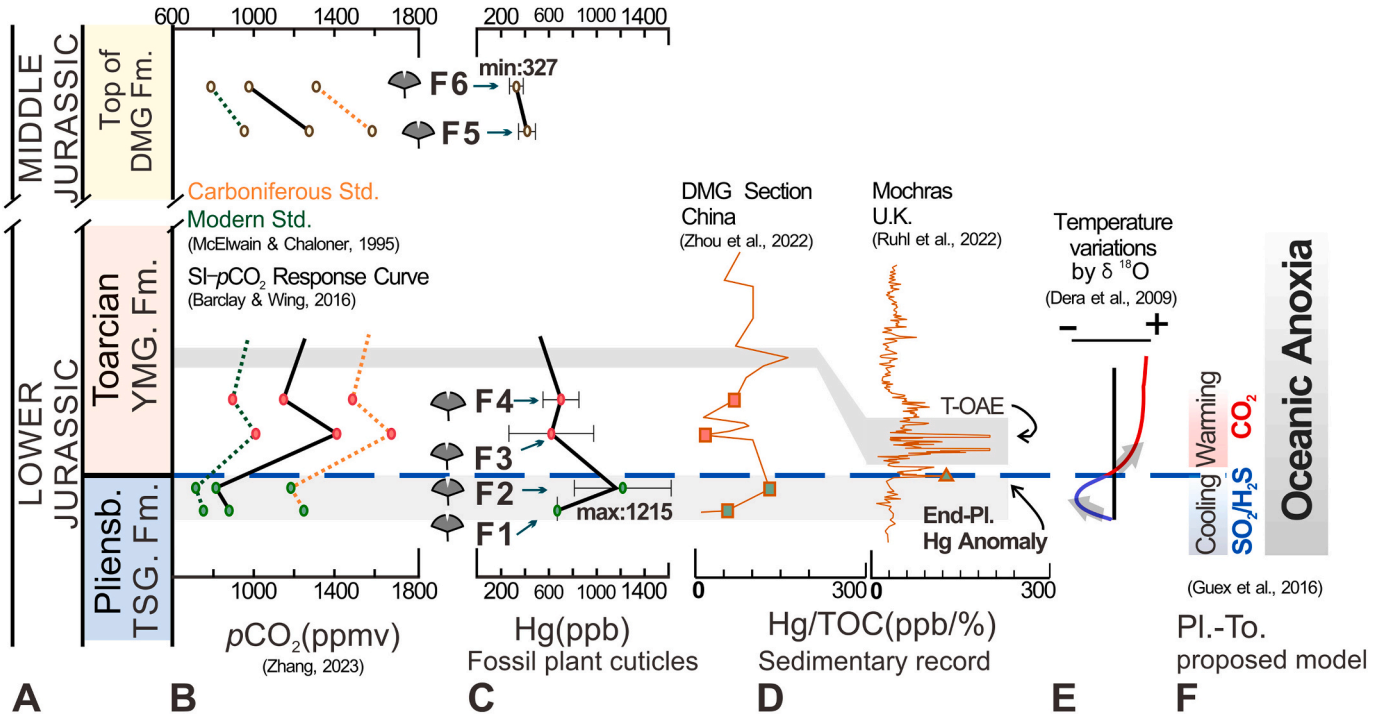

Fig. 7. Chemostratigraphic and fossil cuticle geochemical records for the Lower – Middle Jurassic of the Dameigou Section (Qaidam Basin, China). (A) Stratigraphic information of Dameigou section (Wang et al., 2005); (B) Variations of pCO_2 (ppmv) reconstructed from the fossil ginkgoaleans (Zhang, 2023); (C) Hg content(ppb) in fossil cuticles from the fossil ginkgoaleans (Table 2); (D) Hg/TOC (ppb/%) in sedimentary records, Dameigou data from Zhou et al. (2022), and Monchars data from Ruhl et al. (2022); (E) Temperature variations around the Pliensbachian-Toarcian boundary by Belemnite $\delta^{18}O$ data (Dera et al., 2009); (F) Proposed gas emissions associated to Karoo-Ferrar large igneous province around the Pliensbachian-Toarcian boundary (Guex et al., 2016). *Abbreviations*: Fm, Formation; TSG, Tianshuigou; YMG, Yinmagou; DMG, Dameigou; Pliensb and Pl, Pliensbachian; To, Toarcian; Std, Standard.

the bulk sediment samples in the same section (Lu et al., 2020; Zhou et al., 2022) (Table 2, Fig. 7, D). Cuticles from the lower Toarcian beds F3 and F4, stratigraphically above bed F2, show slightly lower Hg levels, but concentration values overlap within uncertainty, with cucticle-Hg values from beds F1 and F2. Cuticles from the Middle Jurassic beds F5 and F6 show significantly lower Hg levels of ~370 ppb (Fig. 7, C).

Utilizing widely adopted methods for reconstructing palaeo-atmospheric carbon dioxide concentrations (pCO_2) based on plant stomata (Barclay and Wing, 2016; Kürschner, 2001; McElwain and Chaloner, 1995; Steinthorsdottir et al., 2012; Ning Zhou et al., 2020), our previously analysis of fossil ginkgoaleans' stomatal density and inferred palaeo-atmospheric pCO_2 (reported in Zhang, 2023), suggests overall enhanced greenhouse conditions under elevated pCO_2 values of 600–1400 ppmv throughout the Early to Middle Jurassic (Table 2). The lower Toarcian fossil leaf bearing beds F3 and F4 closely precede the T-OAE interval in the Dameigou succession (Li et al., 1988; Wang et al., 2005; Zhang, 2023; Zhang et al., 2023), but suggest a doubling–tripling of palaeo-atmospheric pCO_2 relative to the upper Pliensbachian values inferred form cuticle materials in beds F1 and F2 (Fig. 7, B). Importantly, these results are closely aligned with reconstructed Early Toarcian atmospheric pCO_2 increases based on fossil cuticle analyses from the lower Toarcian succession at Bornholm, Denmark (McElwain et al., 2005). Cooler conditions in the late Pliensbachian, possibly exacerbated by the release of sulfur aerosols during the initial phase of Karoo-Ferrar LIP volcanism (Guex et al., 2016; Tappe et al., 2023), were followed by an early Toarcian 5 °C rise in global seawater temperatures, based on fossil calcite $\delta^{18}O$ data (Dera et al., 2009; Ullmann et al., 2020) (Fig. 7, E), likely directly associated with the observed increase in atmospheric pCO_2 at this time.

Combined, the data suggest that fossil cuticle-Hg levels may be lower during times of elevated atmospheric pCO_2 (Fig. 7), as the lower leaf stomatal density at such times may have negatively impacted on leaf gas exchange rates and associated leaf Hg uptake and sequestration. In detail, these findings are, however, complicated by the very different atmospheric residence times of carbon and Hg, and the low stratigraphic sample resolution of the studied leaf cuticles. Short but intense pulses in volcanic activity may have released both Hg and carbon greenhouse gasses, but Hg would have been sequestered from the atmosphere within years, while carbon greenhouse gasses would have lingered on for 10^4–10^5 times longer.

The preliminary findings presented in this study however provide support for the potential use of stratigraphic variations in fossil cuticle Hg concentrations to serve as indicator of past changes in gaseous Hg levels within the palaeo-atmosphere, and by inference past environmental Hg loading, such as from volcanism. Further studies however warranted, with a specific focus on *Ginkgo biloba*'s response to varied Hg^0 regimes in controlled laboratory settings, Hg migration during fossilization, the Hg species in fossil plant cuticles, and exploration of other macro- or micro-characteristics of plant fossils within the context of significant volcanic events. Through the utilization of multiple proxies, these investigations have the potential to enhance our understanding of the Hg cycle in terrestrial ecosystems, and provide valuable insights into the climatic perturbations associated with volcanic activity in Earth's past.

4. Conclusions

This study presents new data on the Hg content in modern *Ginkgo biloba* leaves, and variations therein i) across the growing season, ii) depending on the position within a tree canopy (e.g., sun/shade leaves), and iii) in response to varying climatic and atmospheric Hg conditions. With this, the study assesses possible abiotic factors influencing foliar Hg concentrations of *Ginkgo biloba*. The study shows that leaf age and local atmospheric Hg concentrations are the two primary factors impacting foliar Hg levels ($p < 0.01$ for both). Additionally, relative humidity and elevation emerged as potential abiotic factors impacting on leaf Hg concentrations (with $p < 0.05$ for both).

The study of cuticle Hg-contents of 23 fossil ginkgoalean samples from six stratigraphic horizons across three formations in the Lower–Middle Jurassic Dameigou sedimentary succession (Qaidam Basin, China), shows fossil cuticles of ginkgoaleans to have higher Hg concentrations (avg. 585.5 $ng \cdot g^{-1}$) compared to the modern *Ginkgo* samples (avg. 61 $ng \cdot g^{-1}$), as well as bulk sediment samples (avg. 113 $ng \cdot g^{-1}$) from the same layers. The high Hg content in fossil plant cuticles is provisionally attributed to both Hg retention and the mass loss of leaves during the fossilization process, which complicates direct comparisons of absolute Hg concentrations in fossil and modern leaf substrates. Nevertheless, the stratigraphic variability in Hg concentrations based on fossil cuticle material from across the Lower and Middle Jurassic, including the Toarcian Oceanic Anoxic Event (T-OAE), may still provide insight into changes in Hg levels in the palaeo-atmosphere, and by inference environmental Hg loading. The obtained fossil cuticle Hg concentration data shows a notable doubling in Hg levels during the onset of Karoo-Ferrar LIP volcanic activity. This observation supports the hypothesis that Hg variations in fossil cuticles have the potential to reflect gaseous Hg changes in the palaeo-atmosphere triggered by palaeo-volcanism.

Further investigations into plant physiology, leaf taphonomy, and the cycle of heavy metals, particularly mercury (Hg) should be considered, to contribute to a deeper understanding of the role of plants in terrestrial ecosystems, the global Hg cycle, and environmental perturbations in Earth's past, especially those associated with major volcanic events.

Supplementary data to this article can be found online at https://doi.org/10.1016/j.palaeo.2024.112214.

CRediT authorship contribution statement

Li Zhang: Writing – original draft, Methodology, Conceptualization. **Yongdong Wang:** Writing – review & editing, Supervision, Resources, Funding acquisition. **Micha Ruhl:** Writing – review & editing, Supervision, Funding acquisition, Conceptualization. **Emma Blanka Kovács:** Writing – review & editing, Methodology, Data curation, Conceptualization. **Yuanyuan Xu:** Methodology, Data curation. **Yanbin Zhu:** Methodology, Data curation. **Ning Lu:** Methodology, Data curation. **Hongyu Chen:** Methodology, Data curation.

Declaration of competing interest

The authors declare that they have no known competing financial interests or personal relationships that could have appeared to influence the work reported in this paper.

Data availability

All data used in the study were available from supplementary materials

Acknowledgements

We sincerely thank Editor Prof. Shuzhong Shen and the reviewers Prof. Jun Shen and Prof. Vivi Vajda for their constructive comments and supportive feedback during the revisions.

We deeply thank Dr. Kai Zhou from Tsinghua University, Prof Ning Tian and Dr. Zhenyu Wu from Shenyang Normal University, Dr. Hui Xu from Yanshan University, Dr. Ziqiang Mao from the Institute of Tibetan Plateau Research at CAS, Dr. Benqi Lu from the Institute of Geochemistry at CAS, and Dr. Zhen Xu from University of Leeds, for their professional assistance in discussion and modern *Ginkgo*/fossil ginkgoalean samples collecting. This study is part of Li Zhang's PhD project, and LZ sincerely thank Prof Jianhua Jin, Prof Yi Wang, Prof Xiaoju Yang, Prof Jian Cao, Prof Yukun Shi, and Prof Defei Yan for their valuable

comments on this study during LZ's PhD viva.

This study was co-sponsored by the National Natural Science Foundation of China (NSFC 42330208, 42488201, 41702004, 41790454, 42002023), the Strategic Priority Research Program (B) of the Chinese Academy of Sciences (XDB26000000), the State Key Laboratory of Palaeobiology and Stratigraphy (20191103, 20192101, 213112), and China Scholarship Council (202006190261). The study links to the ICDP Integrated Understanding of the Early Jurassic Earth System and Timescale (JET) project, and the UNESCO International Geoscience Programs (IGCP) projects 632, 655 and 739.

References

Ariya, P.A., Amyot, M., Dastoor, A., Deeds, D., Feinberg, A., Kos, G., Poulain, A., Ryjkov, A., Semeniuk, K., Subir, M., Toyota, K., 2015. Mercury Physicochemical and biogeochemical transformation in the atmosphere and at atmospheric interfaces: a review and future directions. Chem. Rev. 115, 3760–3802.

Arnold, C.A., 1947. An Introduction to Paleobotany. McGraw-Hill Book Company, New York.

Arnold, J., Gustin, M.S., Weisberg, P.J., 2018. Evidence for nonstomatal uptake of Hg by aspen and translocation of Hg from foliage to tree rings in Austrian Pine. Environ. Sci. Technol. 52, 1174–1182.

Assad, M., Parelle, J., Cazaux, D., Gimbert, F., Chalot, M., Tatin-Froux, F., 2016. Mercury uptake into poplar leaves. Chemosphere 146, 1–7.

Barclay, R.S., Wing, S.L., 2016. Improving the *Ginkgo* CO_2 barometer: Implications for the early Cenozoic atmosphere. Earth Planet. Sci. Lett. 439, 158–171.

Beerling, D.J., McElwain, J.C., Osborne, C.P., 1998. Stomatal responses of the 'living fossil' *Ginkgo biloba* L. to changes in atmospheric CO_2 concentrations. J. Exp. Bot. 49, 1603–1607.

Bergquist, B.A., 2017. Mercury, volcanism, and mass extinctions. Proc. Natl. Acad. Sci. U. S. A. 114, 8675–8677.

Boardman, N.K., 1977. Comparative photosynthesis of sun and shade plants. Annu. Rev. Plant Biol. 28, 355–377.

Cavalcante, L.L., Barbolini, N., Bacsik, Z., Vajda, V., 2023. Analysis of fossil plant cuticles using vibrational spectroscopy: a new preparation protocol. Rev. Palaeobot. Palynol. 316, 104944.

Centre, J.R., Materials, I.F.R., Measurements, Held, A, Perez Przyk, E., 2010. Certification of the Mass Fractions of As, B, Cd, Cr, Cu, Hg, Mn, Mo, Ni, Pb, Sb, Se, Sn and Zn in Rye Grass: Certified Reference Material ERM-CD281 Publications Office.

de Araújo, L.C.A., da Purificação-Júnior, A.F., da Silva, S.M., Lopes, A.C.S., Veras, D.L., Alves, L.C., Dos Santos, F.B., Napoleão, T.H., Dos Santos Correia, M.T., da Silva, M. V., Oliva, M.L.V., de Oliveira, M.B.M., 2019. In vitro evaluation of mercury (Hg(2+)) effects on biofilm formation by clinical and environmental isolates of *Klebsiella pneumoniae*. Ecotoxicol. Environ. Saf. 169, 669–677.

Dera, G., Pellenard, P., Neige, P., Deconinck, J.-F., Pucéat, E., Dommergues, J.-L., 2009. Distribution of clay minerals in early Jurassic Peritethyan seas: palaeoclimatic significance inferred from multiproxy comparisons. Palaeogeogr. Palaeoclimatol. Palaeoecol. 271, 39–51.

Driscoll, C.T., Mason, R.P., Chan, H.M., Jacob, D.J., Pirrone, N., 2013. Mercury as a global pollutant: sources, pathways, and effects. Environ. Sci. Technol. 47, 4967–4983.

El-Sharkawy, M.A., Cock, J.H., Del Pilar Hernandez, A., 1985. Stomatal response to air humidity and its relation to stomatal density in a wide range of warm climate species. Photosynth. Res. 7, 137–149.

Ericksen, J.A., Gustin, M.S., Schorran, D.E., Johnson, D.W., Lindberg, S.E., Coleman, J.S., 2003. Accumulation of atmospheric mercury in forest foliage. Atmos. Environ. 37, 1613–1622.

Feng, X., Li, P., Fu, X., Wang, X., Zhang, H., Lin, C.-J., 2022. Mercury pollution in China: implications on the implementation of the Minamata Convention. Environ Sci Process Impacts 24, 634–648.

Fleck, J.A., Grigal, D.F., Nater, E.A., 1999. Mercury uptake by trees: an observational experiment. Water Air Soil Pollut. 115, 513–523.

Frescholtz, T.F., Gustin, M.S., Schorran, D.E., Fernandez, G.C.J., 2003. Assessing the source of mercury in foliar tissue of quaking aspen. Environ. Toxicol. Chem. 22, 2114–2119.

Fu, X., Feng, X., Zhu, W., Wang, S., Lu, J., 2008. Total gaseous mercury concentrations in ambient air in the eastern slope of Mt. Gongga, South-Eastern fringe of the Tibetan plateau, China. Atmos. Environ. 42, 970–979.

Fu, X., Liu, C., Zhang, H., Xu, Y., Zhang, H., Li, J., Lyu, X., Zhang, G., Guo, H., Wang, X., Zhang, L., Feng, X., 2021. Isotopic compositions of atmospheric total gaseous mercury in 10 Chinese cities and implications for land surface emissions. Atmos. Chem. Phys. 21, 6721–6734.

Gačnik, J., Gustin, M.S., 2023. Tree rings as historical archives of atmospheric mercury: a critical review. Sci. Total Environ. 898, 165562.

Grasby, S.E., Them, T.R., Chen, Z., Yin, R., Ardakani, O.H., 2019. Mercury as a proxy for volcanic emissions in the geologic record. Earth Sci. Rev. 196, 102880.

Graydon, J.A., St. Louis, V.L., Hintelmann, H., Lindberg, S.E., Sandilands, K.A., Rudd, J. W.M., Kelly, C.A., Tate, M.T., Krabbenhoft, D.P., Lehnherr, I., 2009. Investigation of uptake and retention of atmospheric Hg(II) by boreal forest plants using stable Hg isotopes. Environ. Sci. Technol. 43, 4960–4966.

Guex, J., Pilet, S., Müntener, O., Bartolini, A., Spangenberg, J., Schoene, B., Sell, B., Schaltegger, U., 2016. Thermal erosion of cratonic lithosphere as a potential trigger for mass-extinction. Sci. Rep. 6, 23168.

Gustin, M.S., Amos, H.M., Huang, J., Miller, M.B., Heidecorn, K., 2015. Measuring and modeling mercury in the atmosphere: a critical review. Atmos. Chem. Phys. 15, 5697–5713.

Gworek, B., Dmuchowski, W., Baczewska-Dąbrowska, A.H., 2020. Mercury in the terrestrial environment: a review. Environ. Sci. Eur. 32, 1–19.

Hall, G.E., Pelchat, P., 1997. Evaluation of a direct solid sampling atomic absorption spectrometer for the trace determination of mercury in geological samples. Analyst 122, 921–924.

Harris, T.M., 1976. The Mesozoic gymnosperms. Rev. Palaeobot. Palynol. 21, 119–134.

Haworth, M., Belcher, C.M., Killi, D., Dewhirst, R.A., Materassi, A., Raschi, A., Centritto, M., 2018. Impaired photosynthesis and increased leaf construction costs may induce floral stress during episodes of global warming over macroevolutionary timescales. Sci. Rep. 8, 1–14.

Herrick, J.D., Maherali, H., Thomas, R.B., 2004. Reduced stomatal conductance in sweetgum (*Liquidambar styraciflua*) sustained over long-term CO_2 enrichment. New Phytol. 162, 387–396.

Hintelmann, H., Ebinghaus, R., Wilken, R.-D., 1993. Accumulation of mercury (II) and methylmercury by microbial biofilms. Water Res. 27, 237–242.

Hung, K.-N., Yuan, C.-S., Lee, C.-E., Ie, I.-R., Yeh, M.-J., Soong, K.-Y., Fang, S.-C., 2021. Spatiotemporal distribution and long-range transport of atmospheric speciated mercury at three remote islands in Taiwan Strait and South China Sea. Atmos. Res. 248, 105193.

Iniesto, M., Blanco-Moreno, C., Villalba, A., Buscalioni, Á.D., Guerrero, M.C., López-Archilla, A.I., 2018. Plant tissue decay in long-term experiments with microbial mats. Geosciences 8, 387.

Jardine, P.E., Kent, M., Fraser, W.T., Lomax, B.H., 2019. *Ginkgo* leaf cuticle chemistry across changing pCO_2 regimes. PalZ 93, 549–558.

Javelle, M., Vernoud, V., Rogowsky, P.M., Ingram, G.C., 2011. Epidermis: the formation and functions of a fundamental plant tissue. New Phytol. 189, 17–39.

Jin, X., Zhang, F., Baranyi, V., Kemp, D.B., Feng, X., Grasby, S.E., Sun, G., Shi, Z., Chen, W., Dal Corso, J., 2022. Early Jurassic massive release of terrestrial mercury linked to floral crisis. Earth Planet. Sci. Lett. 598, 117842.

Jiskra, M., Sonke, J.E., Obrist, D., Bieser, J., Ebinghaus, R., Myhre, C.L., Pfaffhuber, K.A., Wängberg, I., Kyllönen, K., Worthy, D., Martin, L.G., Labuschagne, C., Mkololo, T., Ramonet, M., Magand, O., Dommergue, A., 2018. A vegetation control on seasonal variations in global atmospheric mercury concentrations. Nat. Geosci. 11, 244–250.

Jones, T.P., Rowe, N.P., 1999. Fossil plants and spores: modern techniques. Geological Society of London, London.

Kovács, E.B., Ruhl, M., Demény, A., Fórizs, I., Hegyi, I., Horváth-Kostka, Z.R., Móricz, F., Vallner, Z., Pálfy, J., 2020. Mercury anomalies and carbon isotope excursions in the western Tethyan Csővár section support the link between CAMP volcanism and the end-Triassic extinction. Glob. Planet. Chang. 194, 103291.

Kovács, E.B., Ruhl, M., McElwain, J., 2022. Leaf fragments as a potential paleo-pHg proxy? [Recorded Poster]. In: Geological Survey Ireland:The 65th Irish Geological Research Meeting (IGRM). Queens University Belfast. Available at: https://www.gsi.ie/documents/Kovacs_IGRM2022.pdf (Accessed 25 February 2022).

Kovács, E.B., Ruhl, M., Silva, R.L., McElwain, J.C., Reolid, M., Korte, C., Ruebsam, W., Hesselbo, S.P., 2024. Mercury sequestration pathways under varying depositional conditions during early Jurassic (Pliensbachian and Toarcian) Karoo-Ferrar volcanism. Palaeogeogr. Palaeoclimatol. Palaeoecol. 637, 111977.

Kürschner, W.M., 2001. Leaf sensor for CO_2 in deep time. Nature 411, 247–248.

Laacouri, A., Nater, E.A., Kolka, R.K., 2013. Distribution and uptake dynamics of mercury in leaves of common deciduous tree species in Minnesota, U.S.A. Environ. Sci. Technol. 47, 10462–10470.

Lange, O.L., Nobel, P.S., Osmond, C.B., Ziegler, H., 1981. Physiological Plant Ecology I: Responses to the Physical Environment. Springer Berlin, Heidelberg.

Li, P., He, Y., Wu, X., Mei, S., Li, B., 1988. Early and Middle Jurassic Strata and their Floras from Northeastern Border of Qaidam Basin, Qinghai. Nanjing University Press, Nanjing.

Li, M., Shao, L., Lu, J., Spiro, B., Wen, H., Li, Y., 2014. Sequence stratigraphy and paleogeography of the Middle Jurassic coal measures in the Yuqia coalfield, northern Qaidam Basin, northwestern China. AAPG Bull. 98, 2531–2550.

Liu, C., Fu, X., Zhang, H., Ming, L., Xu, H., Zhang, L., Feng, X., 2019. Sources and outflows of atmospheric mercury at Mt. Changbai, northeastern China. Sci. Total Environ. 663, 275–284.

Liu, Y., Liu, G., Wang, Z., Guo, Y., Yin, Y., Zhang, X., Cai, Y., Jiang, G., 2022. Understanding foliar accumulation of atmospheric Hg in terrestrial vegetation: progress and challenges. Crit. Rev. Environ. Sci. Technol. 52, 4331–4352.

Locatelli, E.R., McMahon, S., Bilger, H., 2017. Biofilms mediate the preservation of leaf adpression fossils by clays. Palaios 32, 708–724.

Lodenius, M., Tulisalo, E., Soltanpour-Gargari, A., 2003. Exchange of mercury between atmosphere and vegetation under contaminated conditions. Sci. Total Environ. 304, 169–174.

Lomax, B.H., Lake, J.A., Leng, M.J., Jardine, P.E., 2019. An experimental evaluation of the use of $\Delta^{13}C$ as a proxy for palaeoatmospheric CO_2. Geochim. Cosmochim. Acta 247, 162–174.

Lu, J., Zhou, K., Yang, M., Eley, Y., Shao, L., Hilton, J., 2020. Terrestrial organic carbon isotopic composition ($\delta^{13}C_{org}$) and environmental perturbations linked to Early Jurassic volcanism: evidence from the Qinghai-Tibet Plateau of China. Glob. Planet. Chang. 195, 103331.

Lu, Z., Yuan, W., Luo, K., Wang, X., 2021. Litterfall mercury reduction on a subtropical evergreen broadleaf forest floor revealed by multi-element isotopes. Environ. Pollut. 268, 115867.

Manceau, A., Wang, J., Rovezzi, M., Glatzel, P., Feng, X., 2018. Biogenesis of mercury–sulfur nanoparticles in plant leaves from atmospheric gaseous mercury. Environ. Sci. Technol. 52, 3935–3948.
McAusland, L., Vialet-Chabrand, S., Davey, P., Baker, N.R., Brendel, O., Lawson, T., 2016. Effects of kinetics of light-induced stomatal responses on photosynthesis and water-use efficiency. New Phytol. 211, 1209–1220.
McElwain, J.C., 1998. Do fossil plants signal palaeoatmospheric carbon dioxide concentration in the geological past? Philos. Trans. R. Soc. B 353, 83–96.
McElwain, J.C., 2004. Climate-independent paleoaltimetry using stomatal density in fossil leaves as a proxy for CO_2 partial pressure. Geology 32, 1017–1020.
McElwain, J.C., Chaloner, W.G., 1995. Stomatal density and index of fossil plants track atmospheric carbon dioxide in the Palaeozoic. Ann. Bot. 76, 389–395.
McElwain, J.C., Chaloner, W.G., 1996. The fossil cuticle as a skeletal record of environmental change. Palaios 11, 376–388.
McElwain, J.C., Wade-Murphy, J., Hesselbo, S.P., 2005. Changes in carbon dioxide during an oceanic anoxic event linked to intrusion into Gondwana coals. Nature 435, 479–482.
Meyer, H.W., 2003. The Fossils of Florissant Smithsonian Books Washington, DC.
Mosbæk, H., Tjell, J.C., Sevel, T., 1988. Plant uptake of airborne mercury in background areas. Chemosphere 17, 1227–1236.
Murphy, D.M., Hudson, P.K., Thomson, D.S., Sheridan, P.J., Wilson, J.C., 2006. Observations of mercury-containing aerosols. Environ. Sci. Technol. 40, 3163–3167.
Naharro, R., Esbrí, J.M., Amorós, J.A., Higueras, P.L., 2020. Experimental assessment of the daily exchange of atmospheric mercury in *Epipremnum aureum*. Environ. Geochem. Health 42, 3185–3198.
Niu, Z., Zhang, X., Wang, Z., Ci, Z., 2011. Field controlled experiments of mercury accumulation in crops from air and soil. Environ. Pollut. 159, 2684–2689.
Niu, Z., Zhang, X., Wang, S., Ci, Z., Kong, X., Wang, Z., 2013. The linear accumulation of atmospheric mercury by vegetable and grass leaves: potential biomonitors for atmospheric mercury pollution. Environ. Sci. Pollut. Res. 20, 6337–6343.
Obrist, D., Kirk, J.L., Zhang, L., Sunderland, E.M., Jiskra, M., Selin, N.E., 2018. A review of global environmental mercury processes in response to human and natural perturbations: changes of emissions, climate, and land use. Ambio 47, 116–140.
Pacyna, E.G., Pacyna, J.M., Steenhuisen, F., Wilson, S., 2006. Global anthropogenic mercury emission inventory for 2000. Atmos. Environ. 40, 4048–4063.
Pandey, S., Kumar, S., Nagar, P.K., 2003. Photosynthetic performance of *Ginkgo biloba* L. grown under high and low irradiance. Photosynthetica 41, 505–511.
Peckham, M.A., Gustin, M.S., Weisberg, P.J., 2019. Assessment of the suitability of tree rings as archives of global and regional atmospheric mercury pollution. Environ. Sci. Technol. 53, 3663–3671.
Percival, L.M.E., Witt, M.L.I., Mather, T.A., Hermoso, M., Jenkyns, H.C., Hesselbo, S.P., Al-Suwaidi, A.H., Storm, M.S., Xu, W., Ruhl, M., 2015. Globally enhanced mercury deposition during the end-Pliensbachian extinction and Toarcian OAE: a link to the Karoo–Ferrar Large Igneous Province. Earth Planet. Sci. Lett. 428, 267–280.
Pokharel, A.K., Obrist, D., 2011. Fate of mercury in tree litter during decomposition. Biogeosciences 8, 2507–2521.
Rea, A.W., Lindberg, S.E., Scherbatskoy, T., Keeler, G.J., 2002. Mercury accumulation in foliage over time in two northern mixed-hardwood forests. Water Air Soil Pollut. 133, 49–67.
Retallack, G.J., Dilcher, D.L., 2012. Outcrop versus core and geophysical log interpretation of mid-Cretaceous paleosols from the Dakota Formation of Kansas. Palaeogeogr. Palaeoclimatol. Palaeoecol. 329-330, 47–63.
Rex, G.M., 1986. Further experimental investigations on the formation of plant compression fossils. Lethaia 19, 143–159.
Rex, G., Chaloner, W.G., 1983. The experimental formation of plant compression fossils. Palaeontology 26, 231–252.
Riederer, M., Schreiber, L., 2001. Protecting against water loss: analysis of the barrier properties of plant cuticles. J. Exp. Bot. 52, 2023–2032.
Ruhl, M., Hesselbo, S.P., Jenkyns, H.C., Xu, W., Silva, R.L., Matthews, K.J., Mather, T.A., Mac Niocaill, C., Riding, J.B., 2022. Reduced plate motion controlled timing of Early Jurassic Karoo-Ferrar large igneous province volcanism. Sci. Adv. 8, eabo0866.
Rutter, A.P., Schauer, J.J., Shafer, M.M., Creswell, J., Olson, M.R., Clary, A., Robinson, M., Parman, A.M., Katzman, T.L., 2011. Climate sensitivity of gaseous elemental mercury dry deposition to plants: impacts of temperature, light intensity, and plant species. Environ. Sci. Technol. 45, 569–575.
Samuels, L., Kunst, L., Jetter, R., 2008. Sealing plant surfaces: cuticular wax formation by epidermal cells. Annu. Rev. Plant Biol. 59, 683–707.
Schroeder, W.H., Munthe, J., 1998. Atmospheric mercury—an overview. Atmos. Environ. 32, 809–822.
Shen, J., Feng, Q., Algeo, T.J., Liu, J., Zhou, C., Wei, W., Liu, J., Them, T.R., Gill, B.C., Chen, J., 2020. Sedimentary host phases of mercury (Hg) and implications for use of Hg as a volcanic proxy. Earth Planet. Sci. Lett. 543, 116333.
Shen, J., Yin, R., Algeo, T.J., Svensen, H.H., Schoepfer, S.D., 2022a. Mercury evidence for combustion of organic-rich sediments during the end-Triassic crisis. Nat. Commun. 13, 1–8.
Shen, J., Yin, R., Zhang, S., Algeo, T.J., Bottjer, D.J., Yu, J., Xu, G., Penman, D., Wang, Y., Li, L., Shi, X., Planavsky, N.J., Feng, Q., Xie, S., 2022b. Intensified continental chemical weathering and carbon-cycle perturbations linked to volcanism during the Triassic–Jurassic transition. Nat. Commun. 13, 299.
Slater, S.M., Twitchett, R.J., Danise, S., Vajda, V., 2019. Substantial vegetation response to Early Jurassic global warming with impacts on oceanic anoxia. Nat. Geosci. 12, 462–467.
Sokal, R.R., Rohlf, F.J., 1995. Biometry: The Principles and Practices of Statistics in Biological Research, Third ed. W.H. Freeman and Company, New York.
Sprovieri, F., Pirrone, N., Ebinghaus, R., Kock, H., Dommergue, A., 2010. A review of worldwide atmospheric mercury measurements. Atmos. Chem. Phys. 10, 8245–8265.
Sprovieri, F., Pirrone, N., Bencardino, M., D'Amore, F., Angot, H., Barbante, C., Brunke, E.-G., Arcega-Cabrera, F., Cairns, W., Comero, S., 2017. Five-year records of mercury wet deposition flux at GMOS sites in the Northern and Southern hemispheres. Atmos. Chem. Phys. 17, 2689–2708.
Stamenkovic, J., Gustin, M.S., 2009. Nonstomatal versus stomatal uptake of atmospheric mercury. Environ. Sci. Technol. 43, 1367–1372.
Steinthorsdottir, M., Woodward, F.I., Surlyk, F., McElwain, J.C., 2012. Deep-time evidence of a link between elevated CO_2 concentrations and perturbations in the hydrological cycle via drop in plant transpiration. Geology 40, 815–818.
Steinthorsdottir, M., Elliott-Kingston, C., Bacon, K.L., 2018. Cuticle surfaces of fossil plants as a potential proxy for volcanic SO_2 emissions: observations from the Triassic–Jurassic transition of East Greenland. Palaeobiodiv. Palaeoenviron. 98, 49–69.
Steinthorsdottir, M., Jardine, P.E., Lomax, B.H., Sallstedt, T., 2022. Key traits of living fossil *Ginkgo biloba* are highly variable but not influenced by climate – implications for palaeo-pCO_2 reconstructions and climate sensitivity. Glob. Planet. Chang. 211, 103786.
Sun, B., Dilcher, D.L., Beerling, D.J., Zhang, C., Yan, D., Kowalski, E., 2003. Variation in *Ginkgo biloba* L. leaf characters across a climatic gradient in China. Proc. Natl. Acad. Sci. U. S. A. 100, 7141–7146.
Sze, H.C., 1959. Jurassic flora of Qaidam Basin, Qinghai Province, China. Acta Palaeontol. Sin. 8, 3–34.
Tang, B., Chen, J., Wang, Z., Qin, P., Zhang, X., 2021. Mercury accumulation response of rice plant (*Oryza sativa* L.) to elevated atmospheric mercury and carbon dioxide. Ecotoxicol. Environ. Saf. 224, 112628.
Tappe, S., Ngwenya, N.S., Stracke, A., Romer, R.L., Glodny, J., Schmitt, A.K., 2023. Plume–lithosphere interactions and LIP-triggered climate crises constrained by the origin of Karoo lamproites. Geochim. Cosmochim. Acta 350, 87–105.
Taylor, T.N., Taylor, E.L., Michael, K., 2009. Paleobotany: The Biology and Evolution of Fossil Plants., 2nd, Edition ed. Academic Press, Burlington.
Teixeira, D.C., Lacerda, L.D., Silva-Filho, E.V., 2018. Foliar mercury content from tropical trees and its correlation with physiological parameters in situ. Environ. Pollut. 242, 1050–1057.
Travnikov, O., 2005. Contribution of the intercontinental atmospheric transport to mercury pollution in the Northern Hemisphere. Atmos. Environ. 39, 7541–7548.
Ullmann, C.V., Boyle, R., Duarte, L.V., Hesselbo, S.P., Kasemann, S.A., Klein, T., Lenton, T.M., Piazza, V., Aberhan, M., 2020. Warm afterglow from the Toarcian Oceanic Anoxic Event drives the success of deep-adapted brachiopods. Sci. Rep. 10, 6549.
Vajda, V., Pucetaite, M., McLoughlin, S., Engdahl, A., Heimdal, J., Uvdal, P., 2017. Molecular signatures of fossil leaves provide unexpected new evidence for extinct plant relationships. Nat. Ecol. Evol. 1, 1093–1099.
Vajda, V., McLoughlin, S., Slater, S.M., Gustafsson, O., Rasmusson, A.G., 2023. The 'seed-fern' Lepidopteris mass-produced the abnormal pollen *Ricciisporites* during the end-Triassic biotic crisis. Palaeogeogr. Palaeoclimatol. Palaeoecol. 627, 111723.
Vajda, V., McLoughlin, S., Slater, S.M., Gustafsson, O., Rasmusson, A.G., 2024. Confirmation that *Antevsia zeilleri* microsporangiate organs associated with latest Triassic *Lepidopteris ottonis* (Peltaspermales) leaves produced *Cycadopites-Monosulcites-Chasmatosporites*- and *Ricciisporites*-type monosulcate pollen. Palaeogeogr. Palaeoclimatol. Palaeoecol. 640, 112111.
Wang, Y.D., Mosbrugger, V., Zhang, H., 2005. Early to Middle Jurassic vegetation and climatic events in the Qaidam Basin, Northwest China. Palaeogeogr. Palaeoclimatol. Palaeoecol. 224, 200–216.
Wang, Y.D., Huang, C.M., Sun, B.N., Quan, C., Wu, J.Y., Lin, Z.C., 2014. Paleo-CO_2 variation trends and the cretaceous greenhouse climate. Earth Sci. Rev. 129, 136–147.
Wang, Z.X., Sun, F.K., Jin, P.H., Chen, Y.Q., Chen, J.W., Peng, D., Yang, G.L., 2017. A new species of *Ginkgo* with male cones and pollen grains in situ from the Middle Jurassic of eastern Xinjiang, China. Acta Geol. Sin. 91, 9–21.
Wohlgemuth, L., Osterwalder, S., Joseph, C., Kahmen, A., Hoch, G., Alewell, C., Jiskra, M., 2020. A bottom-up quantification of foliar mercury uptake fluxes across Europe. Biogeosciences 17, 6441–6456.
Wohlgemuth, L., Rautio, P., Ahrends, B., Russ, A., Vesterdal, L., Waldner, P., Timmermann, V., Eickenscheidt, N., Fürst, A., Greve, M., Roskams, P., Thimonier, A., Nicolas, M., Kowalska, A., Ingerslev, M., Merilä, P., Benham, S., Iacoban, C., Hoch, G., Alewell, C., Jiskra, M., 2022. Physiological and climate controls on foliar mercury uptake by European tree species. Biogeosciences 19, 1335–1353.
Xie, S., Sun, B., Yan, D., Du, B., 2009. Altitudinal variation in Ginkgo leaf characters: clues to paleoelevation reconstruction. Sci. China Ser. D Earth Sci. 52, 2040–2046.
Xu, Y., Li, Y., Zhou, N., Wang, Y., Lu, N., 2020. Using fossil leaf stomatal parameters to reconstruct the palaeoelevation: method and progress. Acta Palaeon. Sin. 59, 250–263.
Zhang, L., 2023. Exploring the Early–Middle Jurassic Paleoclimate Changes Based on Ginkgophytes Leaf Characteristics: A Case Study of the Dameigou Section in the Qaidam Basin. PhD thesis. School of Earth Sciences & Engineering, Nanjing, China. Nanjing University, 170.
Zhang, H., Li, H., Xiong, C., Zhang, H., Wang, Y., He, Z., Lin, g., Sun, B., 1998. Jurassic Coal-Bearing Strara and Coal Accumulation in Northwest China. Geological Publishing House, Beijing.
Zhang, Y., Jacob, D.J., Horowitz, H.M., Chen, L., Amos, H.M., Krabbenhoft, D.P., Slemr, F., St. Louis, V.L., Sunderland, E.M., 2016. Observed decrease in atmospheric mercury explained by global decline in anthropogenic emissions. Proc. Natl. Acad. Sci. U. S. A. 113, 526–531.

Zhang, L., Yang, T., Li, W.-J., Jia, J.-W., Mou, X.-S., Chen, Y.-Q., Xie, S.-P., Fan, J.-J., Yan, D.-F., 2019. Reading paleoenvironmental information from Middle Jurassic ginkgoalean fossils in the Yaojie and Baojishan basins, Gansu Province, China. Geobios 52, 99–106.

Zhang, H., Fu, X., Yu, B., Li, B., Liu, P., Zhang, G., Zhang, L., Feng, X., 2021. Speciated atmospheric mercury at the Waliguan Global Atmosphere Watch station in the northeastern Tibetan Plateau: implication of dust-related sources for particulate bound mercury. Atmos. Chem. Phys. 21, 15847–15859.

Zhang, L., Wang, Y., Cui, Y., Tian, N., Xie, X., Xie, A., Dong, C., Xi, S., 2022. First fossil foliage record in the red beds from the Upper Jurassic in the Sichuan Basin, southern China. Geol. J. 57, 1628–1637.

Zhang, L., Wang, Y., Ruhl, M., Xu, Y., Zhu, Y., An, P., Chen, H., Yan, D., 2023. Machine-learning-based morphological analyses of leaf epidermal cells in modern and fossil ginkgo and their implications for palaeoclimate studies. Palaeontology 66, e12684.

Zhou, J., Du, B., Shang, L., Wang, Z., Cui, H., Fan, X., Zhou, J., 2020. Mercury fluxes, budgets, and pools in forest ecosystems of China: a review. Crit. Rev. Environ. Sci. Technol. 50, 1411–1450.

Zhou, J., Obrist, D., Dastoor, A., Jiskra, M., Ryjkov, A., 2021. Vegetation uptake of mercury and impacts on global cycling. Nat. Rev. Earth Environ. 2, 269–284.

Zhou, J., Wang, Z., Zhang, X., 2018. Deposition and fate of mercury in litterfall, litter, and soil in coniferous and broad-leaved forests. J. Geophys. Res. Biogeosci. 123, 2590–2603.

Zhou, J., Wang, Z., Zhang, X., Gao, Y., 2017. Mercury concentrations and pools in four adjacent coniferous and deciduous upland forests in Beijing, China. J. Geophys. Res. Biogeosci. 122, 1260–1274.

Zhou, K., Lu, J., Zhang, S., Yang, M., Gao, R., Shao, L., Hilton, J., 2022. Volcanism driven Pliensbachian (early Jurassic) terrestrial climate and environment perturbations. Glob. Planet. Chang. 216, 103919.

Zhou, N., Wang, Y.D., Ya, L., Porter, A.S., Kürschner, W.M., Li, L.Q., Lu, N., McElwain, J. C., 2020. An inter-comparison study of three stomatal-proxy methods for CO_2 reconstruction applied to early Jurassic Ginkgoales plants. Palaeogeog. Palaeoclimatol. Palaeoecol. 542, 109547.

Zhou, N., Xu, Y., Li, L., Lu, N., An, P., Popa, M.E., Kürschner, W.M., Zhang, X., Wang, Y., 2021. Pattern of vegetation turnover during the end-Triassic mass extinction: trends of fern communities from South China with global context. Glob. Planet. Chang. 205, 103585.

Zhou, Z.Y., 1997. Mesozoic ginkgoalean megafossils: a systematic review. In: Hori, T., Ridge, R.W., Tulecke, W., Del Tredici, P., Trémouillaux-Guiller, J., Tobe, H. (Eds.), *Ginkgo biloba* A Global Treasure. Springer, Tokyo, pp. 183–206.

Zhu, H., Zhong, H., Evans, D., Hintelmann, H., 2015. Effects of rice residue incorporation on the speciation, potential bioavailability and risk of mercury in a contaminated paddy soil. J. Hazard. Mater. 293, 64–71.

Zhu, J., Wang, T., Talbot, R., Mao, H., Hall, C.B., Yang, X., Fu, C., Zhuang, B., Li, S., Han, Y., Huang, X., 2012. Characteristics of atmospheric total gaseous mercury (TGM) observed in urban Nanjing, China. Atmos. Chem. Phys. 12, 12103–12118.